THE 8-13 μm SPECTRA OF COMETS AND THE COMPOSITION OF SILICATE GRAINS

Martha S. Hanner
Jet Propulsion Laboratory
Pasadena, CA 91109

David K. Lynch and Ray W. Russell
The Aerospace Corporation
P.O. Box 92957
Los Angeles, CA 90009

July 27, 1993

ABSTRACT

We have analyzed the spectra of seven comets which show an emission feature at 7.8-13 μm. Most have been converted to a common calibration, taking into account the SiO feature in late-type standard stars. The spectra are compared with spectra of the Trapezium, interplanetary dust particles, laboratory mineral samples, and small particle emission models.

The emission spectra show a variety of shapes; there is no unique "cometary silicate". A peak at 11.20-11.25 μm indicative of small crystalline olivine particles, is seen in only three comets of this sample, P/Halley, Bradfield 1987 XXIX, and Levy 1990 XX.

The widths of the emission features range from 2.6 μm - 4.1 μm (FWHM). To explain the differing widths and the broad 9.8 μm maximum, glassy silicate particles, including both pyroxene and olivine compositions, are the most plausible candidates. Calculations of emission models confirm that small grains of glassy silicate well mixed with carbonaceous material are plausible cometary constituents.

No single class of chondritic aggregate IDPs exhibits spectra closely matching the comet spectra. A mixture of IDP spectra, particularly the glass-rich aggregates approximately matches the spectra of P/Halley, Levy, and Bradfield 1987 XXIX. Yet, if comets are simply a mix of IDP types, it is puzzling that the classes of IDPs are so distinct.

None of the comet spectra match the spectrum of the Trapezium. Thus, the mineralogy of the cometary silicates is not the same as that of the interstellar medium. The presence of a component of crystalline silicates in comets may be evidence of mixing between high and low temperature regions in the solar nebula.

THE 8-13 μm SPECTRA OF COMETS AND THE COMPOSITION OF SILICATE GRAINS

I. INTRODUCTION

Comets are the best link we have to the composition of the primitive solar nebula. Study of the dust released from comets and comparison with what we know about the interstellar dust will help to elucidate to what extent interstellar material was reprocessed in the solar nebula. Infrared spectroscopy is ideal for remotely studying the composition of cometary solids. In particular, the 10 μm spectral region (7.8–13.5 μm) contains vibrational mode transitions in common mineral components of the grains. The spectra can help to establish links to interstellar grains and to identify classes of interplanetary dust particles likely to originate from comets. Interplanetary dust particles can be collected at Earth and studied in the laboratory, yielding insight into the formation and processing history of the grains.

A broad emission feature near 10 μm is observed in intermediate bandpass filter photometry of most dynamically new and long-period comets (Ney 1982, Gehrz & Ney 1992). The strength of the feature is quite variable, being strongest in "dust rich" comets with strong scattered light continua at shorter wavelengths.

Spectra at λ 8-13 μm with high signal/noise now exist for nine comets. Four are dynamically new comets, that is, thought to have come in from the Oort cloud for the first time, two are long-period comets, and two (Halley and Brorsen-Metcalf) have periods ~70 years. Additional spectra of several short-period comets allow us to set upper limits to the presence of emission features. In this paper, we analyze these spectra and discuss the composition of the cometary silicates.

II. THE SPECTRA

Cometary spectra have been acquired primarily with three moderate resolution instruments (resolving power ~ 50). The majority of the spectra surveyed here were acquired with a 2% circular variable filter installed in the Si:As photoconductor (AT1) at the NASA Infrared Telescope Facility (IRTF). Because the data are taken sequentially as the CVF is stepped through the desired wavelength range, CVF spectra are vulnerable to tracking errors or changing sky conditions, particularly during daytime. Two comets have been observed from the Kuiper Airborne Observatory with the NASA Ames faint object grating spectrometer (FOGS), which consists of a 24 element Si:Bi linear array (Witteborn & Bregman 1984). The grating position can be moved, allowing the spectrum to be oversampled. The Aerospace Corp. broadband array spectrograph (BASS) spans the wavelength region 2 - 14 μm using two 58-element blocked impurity band linear arrays (Hackwell *et al.* 1990). All spectral elements are observed simultaneously; there are no moving parts.

Two aspects of the data reduction affect the shape of the silicate feature. First, it has recently become clear that the K and M giants usually adopted as standard stars are not, in fact, blackbodies, but have a SiO feature about 14% deep near 8 μm (Cohen *et al.* 1992). While the SiO band does not affect the overall shape of the silicate emission in comets with strong features, it can affect the 8 - 9 μm rising branch and the strength of a weak silicate feature. The spectra of comets OLR, Austin, Levy, Bradfield and Halley at 0.79 AU have been reanalyzed here using the correct spectral shape of the standards.

Second, the continuum flux has to be estimated. This is usually done by fitting a blackbody at the two ends of the spectrum. While the continuum level is usually well-defined at long wavelengths ($\geq$12.5 μm), there is more uncertainty at the short-wavelength side ($\leq$ 8 μm) because the flux of the standard is uncertain due to the SiO band and, at least in some cases, the emission feature may begin to rise at $\lambda \leq 8$ μm. In addition, terrestrial atmospheric extinction can introduce uncertainty at $\lambda \leq 7.9$ μm and within the ozone feature at 9.4 - 9.8 μm, depending on how closely the comet and standard are matched in air mass. For this reason, we present the total flux and adopted continuum for each spectrum, so that the reader may judge the uncertainty.

The comet observations are summarized in Table 1 and are discussed in turn below.

Comet Kohoutek 1973 XII

An 8 - 13 μm spectrum of Comet Kohoutek was acquired with the UCSD CVF spectrometer ($\Delta \lambda/\lambda \sim 0.015$) when the comet was at heliocentric distance r = 0.31 AU preperihelion (Merrill 1974). The standard star was α Boo. The observed flux is plotted in Figure 1*a*. The 600 K blackbody continuum shown in the figure corresponds to the color temperature adopted by Merrill from mid-infrared photometry the previous day.

Comet IRAS-Araki-Alcock 1983 VII

Comet IRAS-Araki-Alcock passed just 0.03 AU from Earth. 8-13 μm spectra of the nucleus and dust coma were obtained at closest approach with the University College London array spectrometer (Hanner *et al.* 1985a). Fig. 1*b* shows the spectrum in the sunward fan 8"W, 3"N of the nucleus. A very weak feature (6-7%) appears when a blackbody continuum is fitted at the two ends of the spectrum. The spectral shape is similar at other positions in the inner coma.

Comet P/Halley 1986 III

Despite the intense observing of Halley, only two high signal/noise 8-13 μm spectra exist. A spectrum was obtained with the FOGS by Bregman *et al.* (1987) on December 17, 1985, at r = 1.25 AU. Standard stars were α Tau and β Gem. The data were combined with a 5-9 μm spectrum obtained 6 days earlier from the Kuiper Airborne Observatory (Figure 1*c*). To define the continuum, we adopt a color temperature of 310 K, fit to the 6 - 7.8 μm

fluxes and to the low point at 12.7 μm. Tokunaga *et al.* (1988) showed that the 5 - 8 μm color temperature of Halley (in this case, 320 K) was about 15% higher than the 8-13 μm color temperature. The dashed line in Fig. 4 corresponds to a color temperature of 290 K. If the long wavelength continuum is really at the level of the 12.2 and 13.2 μm fluxes, then 290 K is a more appropriate continuum level, reducing somewhat the peak height at 11.2 μm.

Campins and Ryan (1989) used the IRTF CVF to obtain a spectrum on January 16 at r = 0.79 AU. The calibration star was β Peg. The Halley fluxes have been recalculated from Campins & Ryan's Table 2, using the revised β Peg spectrum from Hanner *et al.* (1993), which includes the SiO feature. One sees in Figure 1*d* that the revised fluxes (filled circles) are 14% - 5% lower than the original fluxes (open circles) as one moves from λ 8 - 10 μm. Consequently, the best-fit color temperature decreases from 385 K to 360 K; the overall shape of the feature is retained.

Comet Wilson 1987 VII

Comet Wilson, a dynamically new comet, was observed near perihelion at r = 1.20 AU with FOGS from the Kuiper Airborne Observatory (Lynch *et al.* 1989). The spectra were calibrated via α Sco, using a spectrum from Merrill & Stein (1976). The average of three spectra from two flights is displayed in Figure 1*e*. The 5 - 7 μm portion of the spectrum and the points at 12.6 μm can be fit by a 300 K blackbody, about 18% above the equilibrium temperature of 254 K. One sees that the flux is already rising above the continuum at $\lambda \geq$ 7 μm. A temperature a few percent cooler will fit the data from 5-8 μm, but is not consistent with the 12.6 μm flux. The dashed line, corresponding to 315 K, shows the continuum one would define if only a ground-based spectrum at $\lambda \geq$ 7.7μm were available.

Comet Bradfield 1987 XXIX

Two spectra of Bradfield, a long period comet, were obtained with the IRTF CVF. Lynch *et al.* (1988) observed the comet at r = 0.99 AU, a month after perihelion at 0.87 AU (Figure 1*f*). The calibration star was β Peg. Our flux calibration is based on the measured spectrum of β Peg (Hanner *et al.* 1993). Because of the scatter at λ 7.7−8.0 μm, placement of the continuum is uncertain. We adopt T=334 K, fitted to the fluxes at 7.9−8.1 μm and to the 13 μm flux.

The second CVF spectrum, taken at r = 1.45 AU postperihelion, is shown in Figure 1*g* (Hanner *et al.* 1990). A dust model fitted to the photometry at 4.8, 7.8, and 12.5 μm was used to define the continuum; at 8-13 μm the model corresponds to a color temperature of approximately 270 K. The primary standard star was β And and secondary standard was α Tau. Their fluxes were interpolated from their observed magnitudes through the 1-μm wide "silicate" filter set (Hanner *et al.* 1990); this procedure partially accounts for the SiO band.

Comet P/Brorsen-Metcalf 1989 X

Spectra of periodic comet Brorsen-Metcalf were obtained with the IRTF CVF on six mornings at r = 0.6 - 0.5 AU preperihelion (Lynch, Hanner and Russell 1992); α Tau was the primary calibration source. Within 5%, the spectra are smooth black bodies, as shown in Fig. 1*h*.

Comet Okazaki-Levy-Rudenko 1989 XIX

Okazaki-Levy-Rudenko (hereafter OLR) was observed November 5-8, 1989 at r = 0.65 AU with the IRTF CVF (Russell & Lynch (1990). Figure 1*i* shows the average of two spectra from the morning of November 7. The standard star was α Boo. Absolute fluxes of α Boo were derived from spectra of α Boo versus α Lyrae taken with the UKIRT CGS3 spectrometer May 29, 1991 (Hanner & Tokunaga, unpublished). The error bars are the differences of the two spectra from the average. A blackbody T = 370 K fits the fluxes at 8 μm and ≥ 12 μm; a feature ~20% above the continuum is evident.

Comet Austin 1990 V

Austin, another new comet, was observed with the IRTF CVF at r=0.78 AU, after the comet's 0.35 AU perihelion passage (Hanner *et al.* 1993). The calibration was with respect to β Peg, corrected for the SiO band. The average of two spectra is shown in Figure 1*j*. There is some uncertainty in the most appropriate blackbody fit to this spectrum. The equilibrium blackbody temperature at r = 0.78 AU is 315 K, which passes through the data point at 8 μm, when normalized at 12.5 μm. Yet, the data point at 7.8 μm implies a lower continuum, corresponding to a 5% lower color temperature, and we have adopted the lower temperature here.

Comet Levy 1990 XX

Levy was the first comet to be observed with BASS at the IRTF on August 12-15 1990 at r = 1.54 AU preperihelion (Lynch *et al.* 1992). The calibration star was β Peg. Lynch *et al.* assumed β Peg to be a 3500 K blackbody. In this paper, the flux calibration has been redone using the observed spectrum of β Peg from Hanner *et al.* (1993). The August 12 and August 15 spectra are displayed in Figure 1*k*. The new calibration lowers the fluxes several percent between 7.8 μm and 10 μm. On August 15, the feature/continuum ratio is a factor of two lower than on the 12th, although the continuum at $\lambda \geq$ 12.5 μm is unchanged. Color temperatures of 270 K and 250 K fit the continuum on August 12 and 15 respectively.

Spectra of three short-period comets have been published, P/Churyumov-Gerasimenko (Hanner *et al.* 1985b), P/Grigg-Skjellerup (Hanner *et al.* 1984) and P/Schaumasse (Hanner *et al.* 1993). These spectra are indistinguishable from blackbodies, within the errors.

III. THE EMISSION FEATURES

In order to compare the shapes of the emission features, the continuum emission has to be removed. The comet coma is optically thin ($\tau \sim 10^{-5}$); thus, the observed emission is simply the sum of the emission from all the grains within the field of view. The observed flux, F_λ, can be separated into a component arising from "featureless" grains and the flux due to grains having an emission feature

$$F_\lambda \propto \underbrace{\int a^2\, n(a)\, \epsilon_\lambda\,(a)\, B_\lambda\,(T(a))da}_{\text{"featureless"}} + \underbrace{\int a^2\, n'(a)\, \epsilon'_\lambda(a)\, B_\lambda\,(T'(a))da}_{\text{"feature"}} \qquad (1)$$

where a=grain radius, n(a) = dust size distribution, B_λ (T) = Planck function for temperature T, and ϵ_λ = grain emissivity. By "featureless", we mean that ϵ varies only slowly with wavelength. For a size distribution of featureless grains, the emission over limited spectral intervals can be represented by a simple blackbody at color temperature T_c (T_c is not necessarily equal to the physical temperature of the grains because of the broad size distribution and the slow variation of ϵ_λ).

Only small grains, with a relatively narrow size range will produce a feature; therefore we approximate the integral over the size distribution by average quantities. The observed flux is then approximately given by

$$F_\lambda \propto C\ B_\lambda\,(T_c) + C'\,\epsilon_\lambda\ B_\lambda\,(T'_c) \qquad (2)$$

where C and C′ are the total cross sections of featureless and feature−producing grains respectively. Clearly, to obtain the desired parameter, ϵ_λ, the contribution from the featureless grains should be subtracted and the remaining flux divided by the continuum.

Although we do not know *a priori* the relative contribution of the two components, we can make an estimate. The low average albedo of comet dust, the elemental composition of Halley dust measured *in situ*, and the composition of interplanetary dust particles indicate that silicate and carbonaceous material are mixed on a very fine scale; all grains are dark and warm. Models computed using Bruggeman averaged optical constants for a mix of 75% amorphous olivine, 25% glassy carbon by volume (Hanner *et al.* 1992) indicate that, for Halley, Levy, and Bradfield, the featureless grains contribute one-third to one-half of the total flux at 8 μm (see Section IV. B.).

In practice, the continuum is relatively flat at 8 - 13 μm for r ~0.8 -1.5 AU and we find negligible difference in the spectral shape, width, and wavelength of maxima of the cometary emission features derived from the flux-continuum and flux/continuum approaches to the analysis. Rather than subtracting an arbitrary fraction of the flux, we present here the total flux divided by continuum fitted at 7.8 and 13 μm. The absolute strength of the feature/continuum is an indication of the dilution by featureless grains.

Comets Halley, Bradfield, and Levy displayed strong emission features, with a prominent peak at 11.20−11.25 μm as well as a broader maximum near 9.8 μm (Fig. 2*a* - 2*d*). Within

the spectral resolution, the 11.25 μm peak occurs at the same wavelength in all 3 comets. For each of the three comets, similar spectral shape was observed on at least two dates. The relative heights of the 9.8 μm and 11.25 μm maxima depend to some extent on the way the continuum has been defined, particularly for Halley at 1.25 AU, where the continuum level at 13 μm is uncertain (Fig. 2*a*). Although the feature/continuum decreased by a factor of two in Comet Levy from August 12 - 15, the shape of the emission feature was unchanged.

Kohoutek, a new comet, also displayed a strong emission feature (Fig. 2*e*). When the flux is divided by the continuum, the shape is identical to that of Comet Levy. However, a data gap from 10.3 - 11.0 μm leaves it ambiguous whether a peak is actually present near 11 μm. Certainly, the data points at 11.0 and 11.1 μm are not consistent with a peak at 11.25 μm. But, if the 11.25 μm peak is not present, it is interesting that the long-wavelength side of the emission feature is the same as that of the three comets which do have the peak. To test the effect of the continuum on the spectral shape, a 600 K continuum equal to half the total flux at 13 μm ("featureless" grains) was subtracted from the total fluxes and the excess fluxes divided by a 700 K blackbody fit at 8.0 and 13.0 μm. Except for the vertical scaling, the resulting spectrum has the same shape as Fig. 2*e*. The emission feature in Kohoutek does not resemble that of interstellar grains, illustrated in Fig. 2*e* by the Trapezium spectrum, contrary to the statement by Merrill (1974).

Although similar in shape, the emission features in the four comets differ somewhat in their width and the position of the short wavelength rise. The full width at half maximum and the wavelength at half maximum are tabulated in Table 2. The long wavelength decrease of the feature is remarkably similar in all four comets. The flux is down to the continuum level at λ 12.7 μm. However, the location of the rising branch, and consequently the width, differ among the spectra. The width of the feature is not altered more than ~0.1 μm by the method of standard star calibration or the exact placement of the continuum. The widths do not correlate with the strength of the feature (compare Levy on Aug. 12 and 15) or with heliocentric distance (grain temperature). Levy at r=1.54 AU and Kohoutek at r=0.31 AU have the narrowest features. Regardless of where one places the continuum for Halley at 1.25 AU, the emission feature rises at shorter wavelength than the Halley spectrum at 0.79 AU.

New comet Wilson has an emission feature that is broader than those in the other comets (Fig. 2*f*). The feature rises at shorter wavelength, beginning at 7 μm. Even if the continuum is normalized at 7.8 μm, consistent with the treatment of other spectra lacking airborne data, the FWHM is 3.3 μm. The open circles refer to data with uncertain ozone correction. Thus, the true shape of the emission from 9-10 μm is uncertain. While there may be a small dip at 10.7 μm, there is no peak at 11.25 μm within the scatter of the data. Instead, an unusual feature is evident at 12.2 μm, as discussed in Lynch *et al.* (1989).

Austin and OLR are classified as "dust-poor" comets because of the relatively low scattered light continuum at visible wavelengths. Both show weak emission features 10% - 20% above a blackbody continuum fitted near 8 μm and 12.5 μm (Fig. 2*g* and 2*h*). Neither resembles the stronger features discussed above. The emission in Austin rises from 8 μm - 9 μm. There is a flat maximum from 9 μm - 10 μm and a small peak at 11.06 μm, but none at

11.25 μm. The small emission feature in OLR is centered near 11 μm, but is too broad to be the 11.25 μm peak.

P/Brorsen-Metcalf shows the danger of generalizing. With a 70.6 year period and perihelion at 0.48 AU, P/Brorsen-Metcalf has an orbit similar to that of P/Halley and one might have expected their spectra to be similar. The lack of any feature along with only a small temperature excess above an equilibrium blackbody suggests that the grains were larger than those typically present in comets at r < 1 AU. Weak 10 μm emission was apparently present at 0.49 AU postperihelion (Gehrz & Ney 1992).

IV. DISCUSSION

A. Composition Based on Spectral Shape

The 10 μm emission feature is most likely due to the Si-O stretching mode vibration in small silicate particles. Silicates are composed of cosmically abundant elements. Elemental abundances indicative of silicates were common in particles detected by the dust mass spectrometer during the Halley flybys (Jessberger *et al.* 1988). Silicate grains are a major component of interplanetary dust particles (Sandford and Walker 1985). The spectral matches are reasonable, as we discuss here. Excess emission also is observed in comets at 18 - 20 μm, the position of the Si-O bending mode vibration.

Different silicate minerals produce spectral features of differing shape and the spectra of comets Halley, Bradfield, and Levy allow us to say something about the mineralogy of the silicate particles.

11.25 μm peak

The peak at 11.20–11.25 μm in the comet spectra corresponds to the main resonance in crystalline olivine. Fig. 3 compares the Halley spectrum at 0.79 AU with an emission spectrum of ground olivine particles from Stephens & Russell (1979). Not only the peak position, but the long wavelength side of the feature from 11-12 μm corresponds well. The 11.25 μm peak and 11-12 μm slope in Halley also match the spectrum of an olivine IDP (Campins & Ryan 1989).

Other possible explanations for the peak at 11.25 μm, such as SiC or an organic component can be ruled out from the width of the peak, abundance arguments, or for lack of corresponding features, such as the 7.7 and 8.6 μm emission bands present when an 11.3 μm feature is associated with the set of unidentified interstellar emission bands. Moreover, olivine has features in the 20-35 μm region that are remarkably similar to those seen in comet Halley (Zaikowski & Knacke 1975; Herter *et al.* 1987).

Koike *et al.* (1993) have obtained infrared transmission spectra of olivine samples with differing Mg/Fe abundance. They find that the peak lies at 11.3 μm for Mg/(Mg+Fe) = 0.9

and shifts toward 11.5 μm as the Mg abundance decreases. The 11.25 μm position in the comets implies a high Mg/Fe abundance, a conclusion consistent with the dust analyses from the Halley probes (Jessberger *et al.* 1988; Lawler *et al.* 1989).

9.8 μm maximum

To explain the broader maximum near 9.8 μm and the overall width of the cometary features however, another component is required. There are several possibilities:

1) *Mix of crystalline pyroxenes.* Both olivine and pyroxene are high temperature (Mg, Fe) condensates. Pyroxenes display more variety than olivine in their spectral shapes and the peaks are generally shortward of 11 μm. The spectrum of a pyroxene IDP (Sandford & Walker 1985) is compared to comet Levy (the narrowest feature; see Table 2) in Fig. 4. The widths are comparable although the pyroxene spectrum does not have a maximum at 9.8 μm. At least one pyroxene mineral, orthorhombic enstatite, does have a peak at 9.8 μm (Stephens & Russell 1979), although this mineral is not common in IDPs (Bradley *et al.* 1992). Bregman *et al.* (1987) fit their Halley spectrum with a mixture of crystalline olivine and pyroxenes. However, to match the broad width of their spectrum, a component of hydrated silicates was also included.

2) *Anorthite.* Rose (1979) obtained 8-13 μm emission spectra of ground samples of a variety of rock types. He pointed out that anorthite, a high-temperature Ca-Al feldspar, has a broad feature resembling the cometary feature in Kohoutek except for a dip near 9.8 μm. Lunar soil samples, which are rich in anorthite, have a similarly broad feature. Rose found that the 9.8 μm dip was eliminated in an irradiated anorthite sample, giving a better match to Kohoutek than the crystalline sample. Elemental abundances indicative of anorthite were not obvious in the particles sampled by the Halley *in situ* dust analyzer, nor do IDPs contain anorthite.

3) *Glassy silicates.* Glassy, or amorphous, silicate particles generally display broader features with less spectral structure than their crystalline counter-parts. Stephens & Russell (1979) measured the emission spectra of ground and laser vaporized (amorphous) samples of forsterite, a magnesium-rich olivine and enstatite, a magnesium-rich pyroxene. The amorphous olivine emissivity approximately fits the rising side of the feature in Comet Levy and the 9.8 μm peak (Fig. 5). A mixture of amorphous and crystalline olivine could, in principle, create the observed features in Levy and Halley at 0.79 AU. But olivine particles do not emit enough flux at 8 - 9 μm to match Bradfield, Halley at 1.3 AU, or Wilson. Amorphous enstatite, however, has a higher emissivity at 8 - 9 μm (Fig. 5). Other amorphous pyroxenes, such as amorphous bronzite (Dorschner *et al.* 1988) have their peak emission near 9.5 μm. A mixture of amorphous pyroxenes and olivine can produce a short-wavelength rise at the desired position. Glassy quartz could also contribute to the 8 - 9 μm flux (Steyer, Day, & Huffman 1974).

4) *Hydrated silicates.* Layer lattice silicates have a relatively smooth feature that peaks near 9.8 μm (Zaikowski, Knacke and Porco 1975). Type II carbonaceous chondrites have about equal proportions of hydrated silicates and olivine. Their spectra resemble the comet

spectra (Zaikowski & Knacke 1975). The hydrated silicates in carbonaceous chondrites are the result of low-temperature aqueous alteration, presumably in the parent body. Nelson *et al.* (1987) suggested that amorphous silicate grains on the surface of a comet nucleus could be converted to hydrated silicates if exposed to temperatures of 300 K or above for a few weeks. Yet, the silicate feature was strongest in Halley at times of strong jet activity when the silicate dust appeared to be emanating from deep vents in the nucleus, rather than from the surface. Hydrated silicates have a water of hydration feature at 6.2 μm which is not seen in the airborne spectra of Halley and Wilson. Moreover, the Mg/ Fe/Si distribution in carbonaceous chondrites does not resemble the Halley dust particles examined during the spacecraft flybys (Lawler *et al.* 1989).

B. Effect of particle size and shape on the shape of the silicate feature

Figure 6 shows the computed shape of the silicate feature for test particles of radius 0.5, 1.0, and 2.0 μm. The emissivities were computed by Mie theory, using Bruggeman averaged optical constants for a grain consisting of 75% disordered olivine (Krätschmer & Huffman 1979) and 25% glassy carbon (Edoh 1983). Mie theory is adequate to show the general trends when the optical constants vary slowly with wavelength, as is the case for disordered olivine. However, spheres are not a good approximation near a resonance in the optical constants, such as the peak in crystalline olivine (Bohren & Huffman 1983). The fluxes were calculated for T=300 K and the resulting curves were normalized by a blackbody fit at 7.5 and 13 μm, the same procedure followed for the comet spectra.

The width, as well as the height of the feature varies with particle size. However, the position of the rising side remains fairly stable (mid-point of the rising branch is at 9.1 μm for a=0.5 μm, 9.17 μm for a=1.0 μm, 9.25 μm for a=2.0 μm), while the long-wavelength side shifts toward longer wavelength as the particle radius increases (mid-point 10.7 μm for a=0.5μm, 11.2 μm for a=1.0 μm, and 12.75 μm for a=2.0 μm). Thus, while particle size can explain the difference in the strength of the feature among comets, it cannot account for the changing position of the rising branch. Moreover, it is clear that disordered olivine does not provide enough flux at 8 - 9 μm to match the observed cometary spectral features.

Compact grains larger than ~2 μm radius do not produce a strong emission feature. If comet dust consists of fluffy aggregates of submicron grains, then a silicate feature could be produced by considerably larger particles (Hage & Greenberg 1990). The weak emission features in Austin, OLR, and particularly, IRAS-Araki-Alcock imply that small grains are lacking in these comets. Other properties sensitive to particle size such as the scattered light continuum, 3-5 μm thermal emission, 8–13 μm color temperature, and presence of dust tail also correlate with the strength of silicate emission (Gehrz & Ney, 1992; Hanner *et al.* 1993).

The predicted emission from a size distribution of small silicate grains is compared in Fig. 7 with the observed fluxes from Halley at 1.30 AU. The particle emissivities were computed by Mie theory for Bruggeman averaged optical constants for particles composed of 75% glassy bronzite and 25% amorphous carbon. The good agreement in overall strength of the feature and the main maximum near 9.8 μm demonstrates that small grains of glassy

silicates, well mixed with the carbonaceous material, are plausible cometary constituents. The 11.25 μm peak of crystalline olivine cannot be modeled using spherical particles.

Bohren & Huffman (1983) have suggested that a continuous distribution of ellipsoids (CDE) gives a fair approximation to the optical behavior of randomly shaped particles. We use the CDE approximation to illustrate that it takes relatively little material with spectral structure to be visible above a featureless continuum, provided the temperature is the same. Figure 8 shows an example for a Bruggeman averaged mixture of crystalline olivine (optical constants from Steyer, 1974) and glassy carbon. The 11.3 μm feature is apparent even for 10% olivine by volume.

The mass absorption coefficient near the 11.3 μm peak of crystalline olivine is a factor of 3 - 10 times that of amorphous olivine (Day 1974, 1976). Figure 9 shows that, for the CDE approximation, a mixture of approximately 25% crystalline olivine in an amorphous olivine matrix produces roughly equal peak heights at 9.8 μm and 11.3 μm. Thus, only a fraction of the comet grains need to be crystalline.

C. Comparisons with Interplanetary Dust Particles (IDPs)

No doubt, we already have samples of cometary dust among the interplanetary dust particles (IDPs) collected in the stratosphere (Brownlee 1985). The chondritic aggregate IDPs, are fine-grained aggregates of micrometer - submicrometer particles of silicates and carbonaceous material with chondritic abundances of the major rock-forming elements. Their morphology is distinctly different from that of CI and CM meteorites on a similar scale. The chondritic IDPs can be divided into three classes based on their composition and infrared spectra, dominated by pyroxenes, olivine, and layer lattice silicates respectively (Sandford & Walker 1985). The olivine-rich and (particularly) the pyroxene-rich IDPs have a porous structure, while the layer silicate particles have a smoother texture. All three classes are enriched in carbon compared to primitive CI meteorites; the pyroxene-rich IDPs have carbon abundances > 3 x CI (Thomas *et al.* 1993). While one mineral class dominates in each 5-50 μm IDP, other minerals are present in minor amounts; layer silicate grains are seen in anhydrous IDPs (Rietmeijer 1991) and olivine and pyroxene occur in hydrated silicates (Tomeoka 1991). Anorthite is rare. The unequilibrated mineral mixtures, aggregate structure, and high carbon content make the pyroxene IDPs the most "primitive". The wide range in Mg/Fe/Si abundances in the dust particles analyzed during the Halley flybys is similar to that of the pyroxene IDPs, particularly the glass-rich particles (Lawler *et al.* 1989; Bradley *et al.* 1992).

Olivine IDPs show evidence of atmospheric heating, implying fairly high entry velocities, while hydrated IDPs experience minor heating, implying entry velocities ~ 12 km/sec, consistent with prograde circular orbits (Sandford & Bradley 1989). Pyroxene IDPs appear to be intermediate. This dynamical evidence implies an asteroidal origin for the hydrated silicate particles and a cometary origin for the pyroxene and olivine classes, consistent with one's expectations from their morphology and mineralogy.

Rietmeijer and MacKinnen (1985) have found one chondritic porous IDP containing roughly 50% hydrated silicates. The diversity of the layer silicate minerals implies that at least some formed by aqueous alteration, rather than by direct condensation. Rietmeijer (1985) points out that layer silicates exist in dry Antarctic valleys, where chemical alteration of silicate – ice mixtures is aided by the presence of thin water layers between the solid grains and ice down to T ~ 195 K. He proposes that a similar process could have taken place in the IDP parent bodies, including comet nuclei.

No single class of IDPs exhibits an infrared spectrum resembling the cometary spectra shown in this paper. Bregman *et al.* (1987) fit their Halley spectrum with a simple mix of all three IDP classes. The spectra of olivine IDPs match the 11.25 μm peak, but not the overall shape of the cometary feature. The width of the cometary feature in Levy, Kohoutek, and Halley at 0.79 AU is best matched by the pyroxene IDPs (Fig. 4), but they do not show a peak at 9.8 μm. Instead, the pyroxene spectra have two or three peaks between 9 and 11 μm.

Recently, Bradley *et al.* (1992) have identified two very porous aggregates whose spectra are qualitatively similar to the spectra of Halley, Bradfield, and Levy. These IDPs contain abundant glass, along with tiny (<0.1 μm) crystals, mainly enstatite. A few larger (0.1 - 1.0 μm) olivine crystals give rise to a 11.3 μm signature. Bradley *et al.* emphasized that such particles are rare, although they seem to be related to the pyroxene-rich class.

Thus, the link between comet dust and IDPs is ambiguous. If cometary silicates are predominantly glassy, in order to produce the 8–9 μm rise and the broad 9.8 μm maximum, why are glass – rich IDPs relatively rare? Do only the sturdiest IDPs survive? If only the "primitive" pyroxene IDPs are cometary, why do the olivine IDPs have the highest entry velocities? If both olivine and pyroxene IDPs are from comets, why are the two types so distinct? Does this imply that some comets are pyroxene-rich while others are olivine-rich? If so, we should see significant differences among comets in the strength of the 11.25 μm peak.

D. Link to Interstellar Dust

Although cometary silicate particles are often modeled as the silicate cores of interstellar core-mantle particles (e.g. Greenberg & Hage 1990), none of the cometary spectra are the same as the spectra of interstellar silicates. The silicate emission or absorption feature seen in interstellar and circumstellar dust sources has a single broad maximum at 9.8 μm (Fig. 2*e*). The shape is consistent with amorphous, rather than crystalline silicates, particularly amorphous olivine (Day 1974; Stephens & Russell 1979). While the spectra of Halley, Bradfield, Levy, and Kohoutek do display a maximum at 9.8 μm, the width of the cometary emission is broader than that of the Trapezium (Table 2) and the position of the sort-wavelength rise is more variable than one sees in the interstellar medium.

A spectral feature at 11.25 μm due to crystalline olivine is rare in interstellar sources (Aitken *et al.* 1988). Thus, at least some of the original interstellar silicate material must have been reheated. Either the crystalline grains condensed directly from the vapor phase

or amorphous grains were annealed. Did the crystallization take place before or after the grains were incorporated into comet nuclei? Among the existing cometary spectra, no dynamically new comet definitely shows a 11.25 μm peak, although a larger sample of "dusty" new comets needs to be observed before generalizing. Glassy silicates have been annealed into crystalline olivine in the laboratory at T ~ 700 C (Day 1974). At the perihelion distances of Bradfield, Levy, and Halley the temperature of small grains or of the nucleus surface is not hot enough for recrystallization to take place. Perhaps the presence of crystalline olivine particles in comets is evidence for mixing between high and low temperature regions of the solar nebula.

There is no interstellar counterpart to the broad emission feature seen in Comet Wilson, nor to the 12.2 μm peak.

V. CONCLUSIONS

Clearly, there is no single, unique "cometary" silicate. Just three comets observed to date have strong, structured silicate emission (P/Halley and long-period comets Bradfield 1987 XXIX and Levy 1990 XX). Their spectra are remarkably similar, differing only in the position of the short-wavelength rise. These spectra, augmented by information from laboratory analyses of interplanetary dust particles, allow us to draw some conclusions about the cometary silicates. The 11.25 μm peak is due to Mg-rich olivine crystals. Crystalline pyroxenes probably make a major contribution to the 9-11 μm emission. Yet, the pyroxene mineral most common in IDPs (monoclinic clinoenstatite; Bradley *et al.* 1992) does not have an obvious 9.8 μm maximum. Thus, glassy silicate particles are probably present in the comet dust and, indeed, the glass-rich porous IDPs provide the best match to the cometary spectra, as well as matching the range in Mg/Fe/Si detected in Halley dust. Variations in the abundance and composition of the glassy particles (e.g. pyroxene/olivine/quartz...) may explain the differences among the comet spectra at 8-9 μm. That the relative strengths of the 9.8 and 11.3 μm peaks are similar in the three comets implies that a similar mineral mix is present. Hydrated silicates are not ruled out by the infrared spectra, but IDPs that are predominantly hydrated have low atmospheric entry velocities, implying an asteroidal origin.

In contrast, the very broad, structureless emission feature in new comet Wilson is difficult to explain with the mineral mixtures described above. A mixture of amorphous materials with a wide range in composition appears the most likely alternative. The sharp peak at 12.2 μm remains a mystery.

Weak or absent silicate emission in several of the comets can best be explained by a dust size distribution weighted towards larger particles, since silicate particles larger than a few micrometers do not produce an obvious emission peak. These comets have a relatively low dust scattering continuum at visible wavelengths. Moreover, the 3 μm thermal continuum is also low, indicating that small, hot grains are lacking. Why the size distribution differs is not known; both new and evolved comets fall in this category, so that thermal alteration of the nucleus surface is not a sufficient explanation.

The cometary emission features do not match the spectrum of the Trapezium, although the 9.8 μm maximum in Halley, Levy, Bradfield, and Kohoutek could be related to the interstellar feature. At least some of the silicate material in comets has been strongly heated to produce crystalline grains. The heating must have taken place before the grains were incorporated into comet nuclei. If, as we believe, the comet nuclei formed in regions not subjected to significant heating, then we may be seeing evidence of mixing between high and low temperature regions of the solar nebula.

Have we seen the full range of cometary spectra? Probably not! The four new comets observed to date each have a unique spectrum. None shows a 11.25 μm peak, although the spectrum of Kohoutek is ambiguous. Two of the four have only weak emission features. We know from photometry that many new comets do have strong silicate emission. We need to obtain more spectra of these comets before we can conclude whether 11.25 μm olivine emission is lacking in new comets.

It is puzzling that the olivine-rich and pyroxene-rich IDPs have distinctly different morphologies, mineralogies, and entry velocities. If both classes originate from comets, why are they so different? Does this imply that different comets may be more pyroxene-rich or olivine-rich depending on their region of origin? Only a larger sample of cometary spectra will allow us to answer this question.

ACKNOWLEDGEMENTS

This research was carried out in part at the Jet Propulsion Laboratory, California Institute of Technology, under contract with the National Aeronautics and Space Administration (Planetary Astronomy Program). The work at the Aerospace Corporation was supported by the Aerospace Sponsored Research program.

Table 1. 8-13 μm Spectra of Comets

Comet	q AU	r AU	Δ AU	FOV arcsec	Instrument	Reference
Kohoutek 1973 XII	0.14	0.31	1.1	22	CVF	Merrill (1974)
IRAS-Araki-Alcock 1983 VII	0.99	1.00	0.03	4.2	UCL[a]	Hanner et al (1985)
Halley 1986 III	0.59	1.25	0.86	21	FOGS	Bregman et al (1987)
Halley 1986 III	0.59	0.79	1.42	8.2	CVF	Campins & Ryan (1989)
Wilson 1987 VII	1.20	1.20	0.66	21	FOGS	Lynch et al (1989b)
Bradfield 1987 XXIX	0.87	0.99	0.85		CVF	Lynch et al (1989a)
Bradfield 1987 XXIX	0.87	1.45	1.10	7	CVF	Hanner et al (1990)
Brorsen-Metcalf 1989X	0.48	0.6–0.5	0.85–1.0	7,9.5	CVF	Lynch et al (1992a)
Okazaki-Levy-Rudenko 1989 XIX	0.64	0.65	0.88	9.5	CVF	Russell & Lynch (1990)
Austin 1990 V	0.35	0.78	0.46	9.4	CVF	Hanner et al (1993)
Levy 1990 XX	0.94	1.54	0.6	3.7	BASS	Lynch et al (1992b)

a: array spectrometer, University College London

Table 2. Width of the 10 μm Emission Feature

Comet	1 Type	2 R (AU)	3 FWHM (μm)	4 λ_1 (μm)	5 λ_2 (μm)
Levy	L	1.56	2.6	9.05	11.65
Levy	L	1.51	2.75	8.95	11.7
Kohoutek	N	0.31	2.75	9.05	11.8
Halley	P	0.79	2.8	8.85	11.65
Bradfield	L	0.99	2.85	8.85	11.7
Bradfield	L	1.45	2.9	8.7	11.6
Halley	P	1.25	3.15	8.6	11.75
Wilson	N	1.20	4.1*	8.2	12.3*
			3.7#	8.2	11.9#
Trapezium+			2.5	8.9	11.4

1 N=new; L=Long period; P=short period
2 R: heliocentric distance
3 full width at half maximum
4 λ_1 = midpoint, short-λ wing
5 λ_2 = midpint, long-λ wing
* including 12.2 μm peak
\# underdrawing 12.2 μm peak
\+ Trapezium spectrum from Forrest et al (1975) divided by 250 K continuum.

REFERENCES

Aitken, D. K., Roche, P. F., Smith, C. H., James, S. D., and Hough, J. H. 1988. Infrared spectropolarimetry of AFGL 2591: evidence for an annealed grain component. M.N.R.A.S. 230, 629.

Bohren, C. F. and Huffman, D. R. 1983. Absorption and Scattering of Light by Small Particles. John Wiley & Sons, New York.

Bradley, J. P., Humecki, H. J., and Germani, M. S. 1992. Combined infrared and analytical electron microscope studies of interplanetary dust particles. Ap.J. 394, 643-651.

Bregman, J., Campins, H., Witteborn, F.C., Wooden, D.H., Rank, D.M., Allamandola, L.J., Cohen, M., and Tielens, A.G.G.M. 1987. Airborne and Groundbased Spectrophotometry of Comet P/Halley from 5-13 μm. A & A 187, 616-620.

Brownlee, D. E. 1985. Cosmic dust: collection and research. Ann. Rev. Earth Plan. Sci. 13, 147-173.

Campins, H., and Ryan, E. 1989. The identification of crystalline olivine in cometary silicates. Ap. J. 341, 1059-1066.

Cohen, M., Witteborn, F. C., Carbon, D. F., Augason, G., Wooden, D., Bregman, J. and Goorvitch, D. 1992. Spectral irradiance calibration in the infrared III. The influence of CO and SiO. AJ 104, 2045-2052.

Day, K. L. 1974. A possible identification of the 10-micron "silicate" feature. Ap.J. Lett. 192, L15-L17.

Day, K. L. 1976. Further measurements of amorphous silicates. Ap.J. 210, 614-617.

Dorschner, J., Friedemann, C., Gürtler, J., Henning, Th. & Wagner, H. 1986. Amorphous bronzite - a silicate of astronomical importance. MNRAS 218, 37p-40p.

Dorschner, J., Friedemann, C., Gürtler, J., Henning, Th. 1988. Optical properties of glassy bronzite and the interstellar silicate bands. A & A 198, 223-232.

Edoh, O. 1983. Ph.D. dissertation, University of Arizona. Quoted in Hanner, M. S. 1988. Infrared Observations of Comets Halley and Wilson and Properties of the Grains, NASA CP 3004, p. 26.

Forrest, W. J., Gillett, F. C., and Stein, W. A. 1975. Circumstellar grains and the intrinsic polarization of starlight. ApJ. 195, 423-440.

Gehrz, R. D., and Ney, E. P. 1992. 0.7 to 23 μm photometric observations of P/Halley 1986 III and six recent bright comets. Icarus 100, 162-186.

Greenberg, J. M. and Hage, J. I. 1990. From interstellar dust to comets: a unification of observational constraints. ApJ 361, 260-274.

Hackwell, J. A., Warren, D. W., Chatelain, M., Dotan, Y., Li, P., Lynch, D. K., Mabry, D., Russell, R. W., and Young, R. 1990. A low resolution array spectrograph for the 2.9–13.5 μm spectral region. *Proc. SPIE Conference 1235 on Instrumentation in Astronomy VII*, Vol. 1235, pp. 171–180.

Hage, J. I. and Greenberg, J. M. 1990. A model for the optical properties of porous grains. ApJ. 361, 251-259.

Hanner, M. S., Aitken, D. K., Knacke, R., McCorkle, S., Roche, P. F. and Tokunaga, A. T. 1985a. Infrared spectrophotometry of Comet IRAS-Araki-Alcock (1983d): A bare nucleus revealed? Icarus 62, 97-109.

Hanner, M. S. Aitken, D. K., Roche, P. and Whitmore, B. 1984. A search for the 10-micron silicate feature in periodic comet Grigg-Skjellerup. AJ 89, 170-171.

Hanner, M.S., Lynch, D. K. and Russell, R. W. 1993. The 8-13 μm spectrum of comet P/Schaumasse. In preparation.

Hanner, M.S., Newburn, R.L., Gehrz, R.D., Harrison, T., Ney, E.P., and Hayward, T.L. 1990. The infrared spectrum of comet Bradfield (1987s) and the silicate emission feature. Ap. J. 348, 312-321.

Hanner, M.S., Russell, R. W., Lynch, D. K. and Brooke, T. Y. 1993. Infrared spectroscopy and photometry of comet Austin 1990 V. Icarus 101, 69-275.

Hanner, M. S., Tedesco, E. Tokunaga, A. T., Veeder, G. J., Lester, D. F., Witteborn, Bregman, J. D., Gradie, J., and Lebofsky, L. 1985b. The dust coma of periodic comet Churyumov-Gerasimenko (1982 VIII). Icarus 64, 11-19.

Hanner, M. S., Veeder, G. J., and Tokunaga, A. T. 1992. The dust coma of comet P/Giacobini-Zinner in the infrared. A. J. 104, 386-393.

Herter, T., Campins, H. and Gull, G. E. 1987. Airborne spectrophotometry of P/Halley from 16 to 30 microns. A & A 187, 629-631.

Jessberger, E. K., Christoforidis, A., and Kissel, J. 1988. Aspects of the major element composition of Halley's dust. Nature 332, 691.

Krätschmer, W. and Huffman, D. R. 1979. Infrared extinction of heavy ion irradiated and amorphous olivine with application to interstellar dust. Astrophys. Space Sci. 61, 195.

Koike, C., Shibai, H., Tuchiyama, A. 1993. Extinction of olivine and pyroxene in mid- and far infrared regions. M.N.R.A.S., in press.

Lawler, M.E., Brownlee, D.E., Temple, S. & Wheelock, M.M. 1989. Iron, magnesium, and silicon in dust from comet Halley. Icarus 80, 225-242.

Lynch, D. K., Hanner, M. S. and Russell, R. W. 1992. 8-13 μm Spectroscopy and IR Photometry of Comet P/Brorsen-Metcalf (1989o) near Perihelion. Icarus 97, 269-275.

Lynch, D. K., Russell, R. W. and Campins, H. 1988. 10μm spectral structure in comets. Interstellar Dust: Contributed Papers. IAU Symposium #135, 26-30 July, 1988, NASA CP-3036, 417-422.

Lynch, D. K., Russell, R. W., Campins, H., Witteborn, F. C., Bregman, J. D., Rank, D. W., and Cohen, M. C. 1989. 5-13 μm Airborne Observations of Comet Wilson 1986 l. Icarus 82, 379-388.

Lynch, D.K., Russell, R.W., Hackwell, J.A., Hanner, M.S., and Hammel, H.B. 1992. 8-13 μm Spectroscopy of Comet Levy 1990 XX. Icarus 100, 197-202.

Merrill, K. M. 1974. 8-13 μm Spectrophotometry of Comet Kohoutek. Icarus 23, 566-567.

Merrill, K. M. and Stein, W. A. 1976. 2-14 μm stellar spectrophotometry I. Stars of the conventional spectral sequence. PASP 88, 285-293.

Nelson, R., Nuth, J. A. and Donn, B. 1987. Proc. 17th Lunar Planetary Sci. Conf., JGR 92, p. E657.

Ney, E.P. 1982. Optical and Infrared Observations of Bright Comets in the Range 0.5 μm to 20 μm. In Comets, ed. L.L. Wilkening, Univ. Arizona Press, Tucson, 323-340.

Rietmeijer, F. J. M. 1985. A model for diagenesis in proto-planetary bodies. Nature 313, 293-294.

Rietmeijer, F. J. M. 1991. Aqueous alteration in five chondritic porous interplanetary dust particles. Earth and Plan. Sci. Lett. 102, 148-157.

Rietmeijer, F. J. M. and MacKinnon, I.D.R. 1985. Layer silicates in a chondritic porous interplanetary dust particle. JGR 90, D149-D155.

Rose, L. A. 1979. Laboratory simulation of infrared astrophysical features. Astrophys. Space Sci. 65, 47-67.

Russell, R. W. and Lynch, D. K. 1990. Silicates and variability in comets Okazaki-Levy-Rudenko (1989r) and Austin (1989 cl). In Workshop on Observations of Recent Comets (1990), ed. W. F. Huebner, J. Rahe, P. A. Wehinger, I. Konno, p. 92-96.

Sanford, S. A., and Bradley, J. P. 1989. Interplanetary dust particles collected in the stratosphere: observations of atmospheric heating and constraints on their interrelationships

and sources. Icarus 82, 146-166.

Sandford, S.A., and Walker, R.M. 1985. Laboratory infrared transmission spectra of individual interplanetary dust particles from 2.5 to 25 microns. Ap. J. 291, 838-851.

Stephens, J.R., and Russell, R.W. 1979. Emission and extinction of ground and vapor-condensed silicates from 4 to 14 microns and the 10 micron silicate feature. Ap. J. 228, 780-786.

Steyer, T. R. 1974. Infrared properties of some solids of possible interest in astronomy and atmospheric physics. Ph.D. dissertation. University of Arizona.

Steyer, T. R., Day, K. L. and Huffman, D. R. 1974. Infrared absorption by small amorphous quartz spheres. Appl. Opt. 13, 1586-1590.

Thomas, K. L., Blanford, G. E., Keller, L. P., Klöck, W. and McKay D. S. 1993. Carbon abundance and silicate mineralogy of anhydrous interplanetary dust particles. Geochim. Cosmochim. Acta 57, 1551-1566.

Tokunaga, A.T., Golisch, W.F., Griep, D.M., Kaminski, C.D., and Hanner, M.S. 1988. The NASA Infrared Telescope Facility Comet Halley Monitoring Program. II. Postperihelion Results. Astron. J. 96, 1971-1976.

Tomeoka, K. 1991. Aqueous alteration in hydrated interplanetary dust particles. In Origin and Evolution of Interplanetary Dust, (A. C. Levasseur-Regourd & H. Hasegawa, eds.) pp.71-78.

Warren, D. W. and Hackwell, J. A. 1989. A compact prism spectrograph suitable for broadband infrared spectral surveys with array detectors. SPIE 1155, 314-321.

Witteborn, F. C. and Bregman, J. D. 1984. Proc. SPIE 509, 123.

Zaikowski, A. and Knacke, R. F. 1975. Infrared spectra of carbonaceous chondrites and the composition of interstellar grains. Astrophys. Space Sci. 37, 3-9.

Zaikowski, A., Knacke, R. F. and Porco, C. C. 1975. On the presence of phyllosilicate minerals in the interstellar grains. Astrophys. Space Sci. 35, 97-115.

Figure Legends

Figure 1*a*: Comet Kohoutek, observed fluxes and 600 K blackbody (Merrill 1974).

Figure 1*b*: Comet IRAS-Araki-Alcock, observed fluxes at position 8"W, 3"N of nucleus (Hanner et al 1985). — 277 K blackbody.

Figure 1*c*: Comet Halley, observed fluxes 12 and 17 Dec. 1985 (Bregman et al 1987). — 310 K blackbody, --- 290 K blackbody.

Figure 1*d*: Comet Halley, observed fluxes 16 Jan. 1986 (Campins & Ryan 1989). o fluxes from Campins & Ryan, • revised fluxes based on β Peg spectrum, — 360 K blackbody.

Figure 1*e*: Comet Wilson, observed fluxes (Lynch et al 1989). — 300 K blackbody --- 314 K blackbody.

Figure 1*f*: Comet Bradfield, observed fluxes 3 Dec. 1987 (Lynch et al 1989) — 334 K blackbody.

Figure 1*g*: Comet Bradfield, observed fluxes 13 Jan. 1988 (Hanner et al 1990). — dust model (T~ 270 K).

Figure 1*h*: Comet P/Brorsen-Metcalf, observed fluxes (Lynch et al 1992).

Figure 1*i*: Comet Okazaki-Levy-Rudenko, average of two CVF spectra (Russell & Lynch 1990). — 370 K blackbody.

Figure 1*j*: Comet Austin, observed fluxes (Hanner et al 1992). • CVF spectrum, ▲ silicate filters, — 300 K blackbody, --- 315 K blackbody.

Figure 1*k*: Comet Levy, observed fluxes (Lynch et al 1992). • 12 Aug. 1990, ■ 15 Aug. 1990, — 270 K blackbody, --- 250 K blackbody.

Figure 2*a*: Comet Halley, r=1.3 AU. • total fluxes / 310 K blackbody continuum, --- total fluxes / 290 K continuum.

Figure 2*b*: Comet Halley, r=0.79 AU. o total fluxes from Campins & Ryan / 385 K continuum, • fluxes based on β Peg spectrum / 360 K continuum.

Figure 2*c*: Comet Bradfield, • r=0.99 AU total fluxes/ 335 K continuum, ▲ r=1.45 AU total fluxes / dust model.

Figure 2*d*: Comet Levy, 12 Aug. 1990, total fluxes / 266 K continuum.

Figure 2*e*: Comet Kohoutek, total fluxes / 600 K continuum. — Trapezium (Forrest *et al.* 1975) / 250 K continuum, scaled to Kohoutek.

Figure 2*f*: Comet Wilson, total fluxes / 300 K continuum. Open circles are data points affected by terrestrial ozone absorption.

Figure 2*g*: Comet Austin, total fluxes / 300 K continuum (Hanner et al 1993).

Figure 2*h*: Comet Okazaki-Levy-Rudenko, total fluxes / 370 K continuum.

Figure 3: The 11.25 μm olivine feature. • measured emissivity of ground olivine (Stephens & Russell 1979) — Halley flux/ continuum at r=0.79 AU from Fig. 2*b*.

Figure 4: Crystalline pyroxene spectrum compared to comet Levy. — Levy flux/continuum from Fig. 2*d*, • pyroxene IDP "Key" (Sandford & Walker 1985), inverted transmission spectrum with arbitrary vertical scaling.

Figure 5: Emissivity of amorphous silicates. — laser vaporized olivine, --- laser vaporized enstatite (Stephens & Russell 1979), with arbitrary vertical scaling. ■ Bradfield, r=0.99 AU (Fig. 2*c*), • Levy (Fig. 2*d*).

Figure 6: Computed shape of the silicate feature for grains composed of 75% disordered olivine and 25% glassy carbon.

Figure 7: Dust model for size distribution of grains composed of 75% glassy bronzite and 25% glassy carbon. • Total fluxes for Halley at 1.3 AU from Fig. 1*c*.

Figure 8: Average cross section per unit volume for mixtures of carbon and crystalline olivine in the CDE approximation. — 50% olivine, --- 25% olivine, ... 15% olivine, 10% olivine.

Figure 9: Average cross section per unit volume for mixtures of amorphous and crystalline olivine in the CDE approximation. — 50% crystalline, --- 25% crystalline, 10% crystalline.

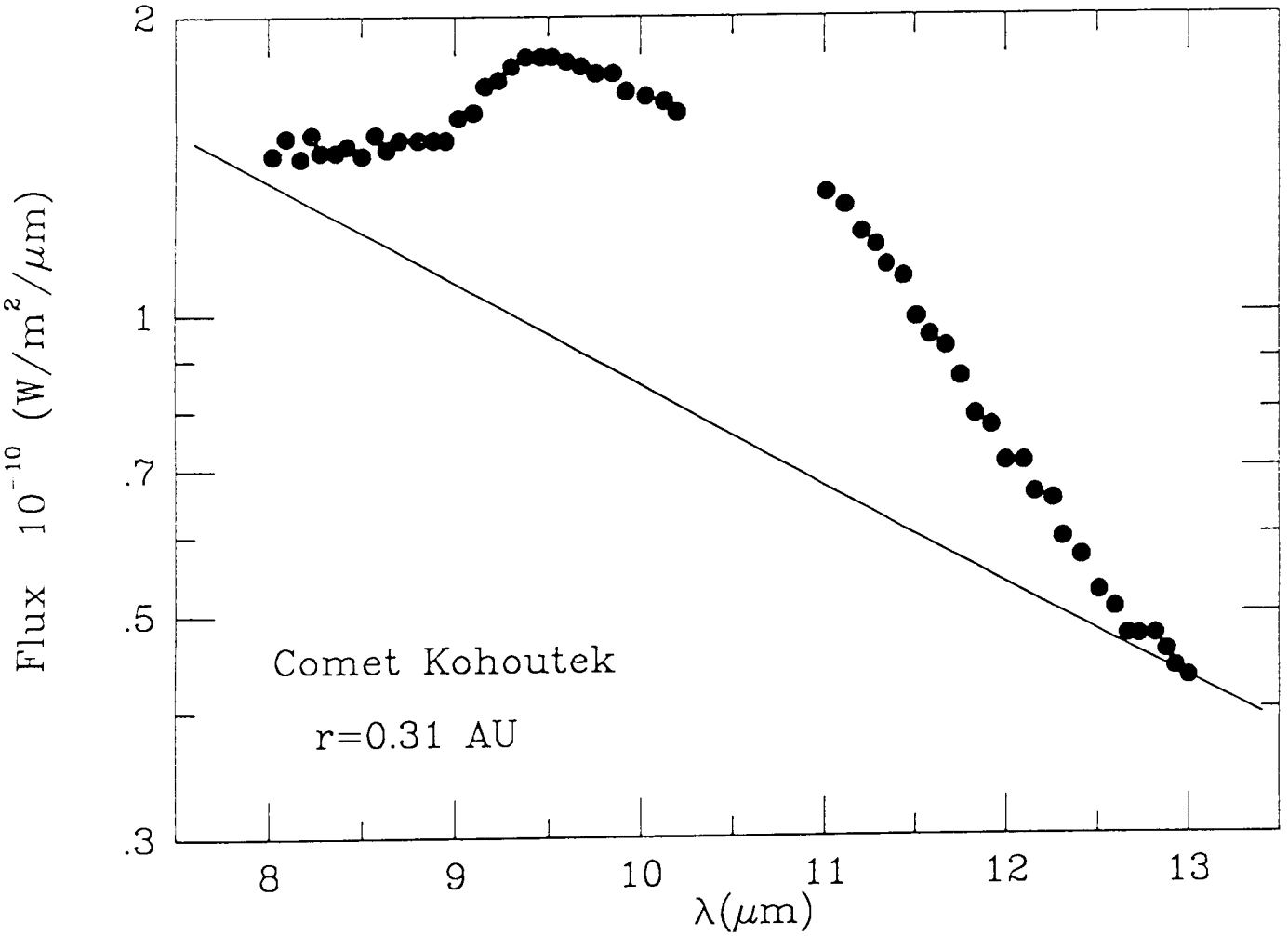
Flux 10^{-10} (W/m^2/μm)
2
1
.7
.5
.3
Comet Kohoutek
r=0.31 AU
8
9
10
11
12
13
$\lambda(\mu m)$

Fig. 1a

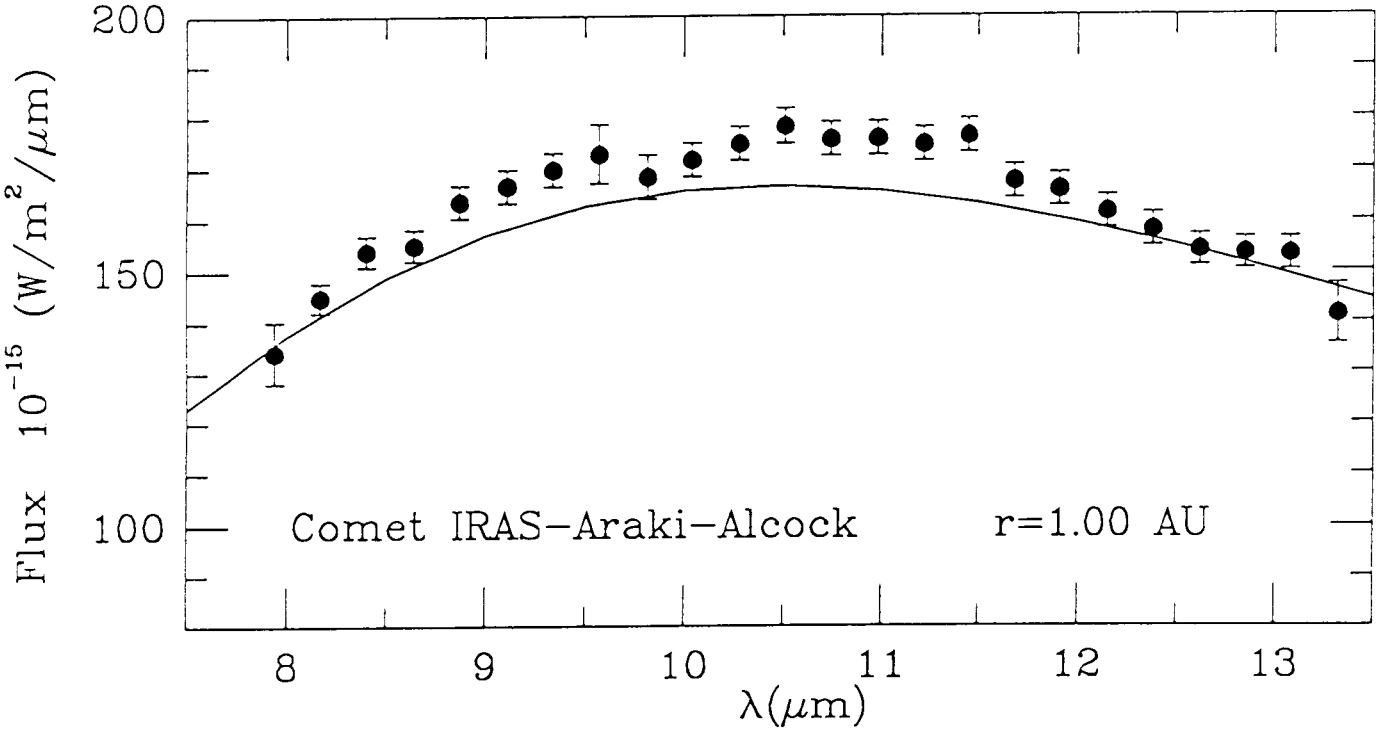
200
150
100
Flux 10^{-15} (W/m^2/μm)
Comet IRAS-Araki-Alcock
r=1.00 AU
8
9
10
11
12
13
$\lambda(\mu m)$

Fig. 1b

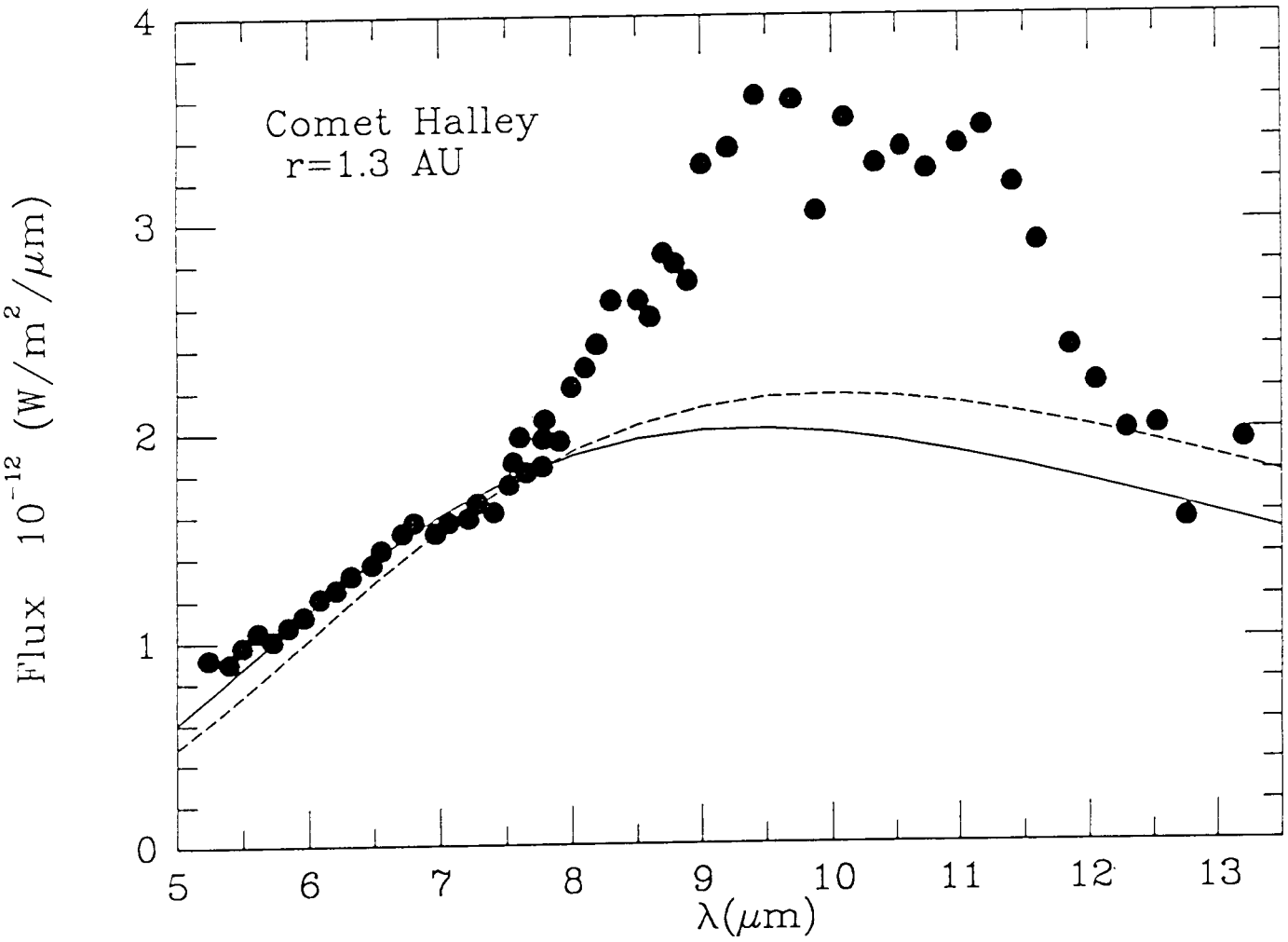
Comet Halley
r=1.3 AU
Flux 10^{-12} (W/m^2/μm)
$\lambda(\mu m)$
0
1
2
3
4
5
6
7
8
9
10
11
12
13

Fig. 1c

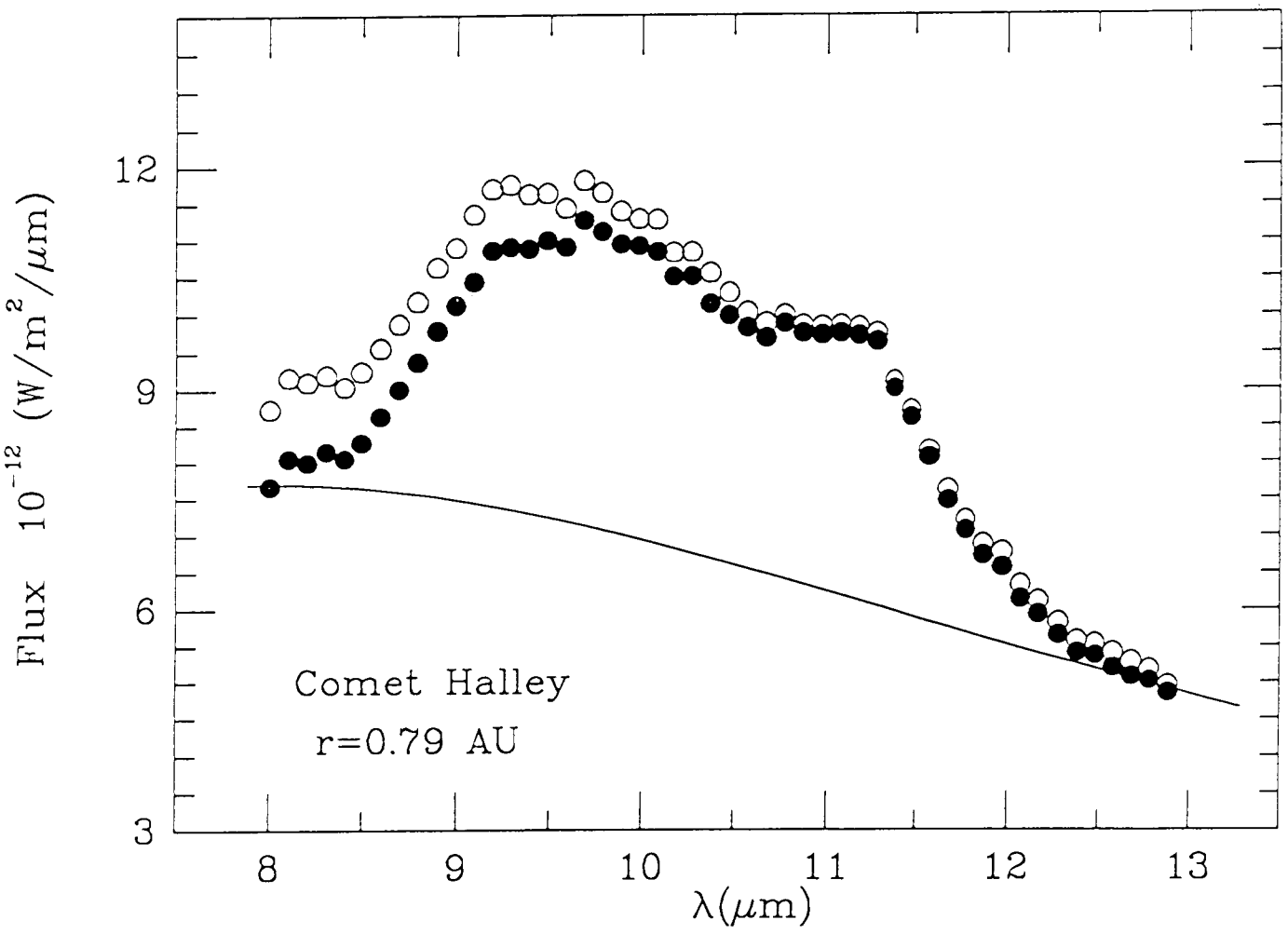
Flux 10^{-12} (W/m^2/μm)
12
9
6
3
8
9
10
11
12
13
$\lambda(\mu m)$
Comet Halley
r=0.79 AU

Fig. 4a

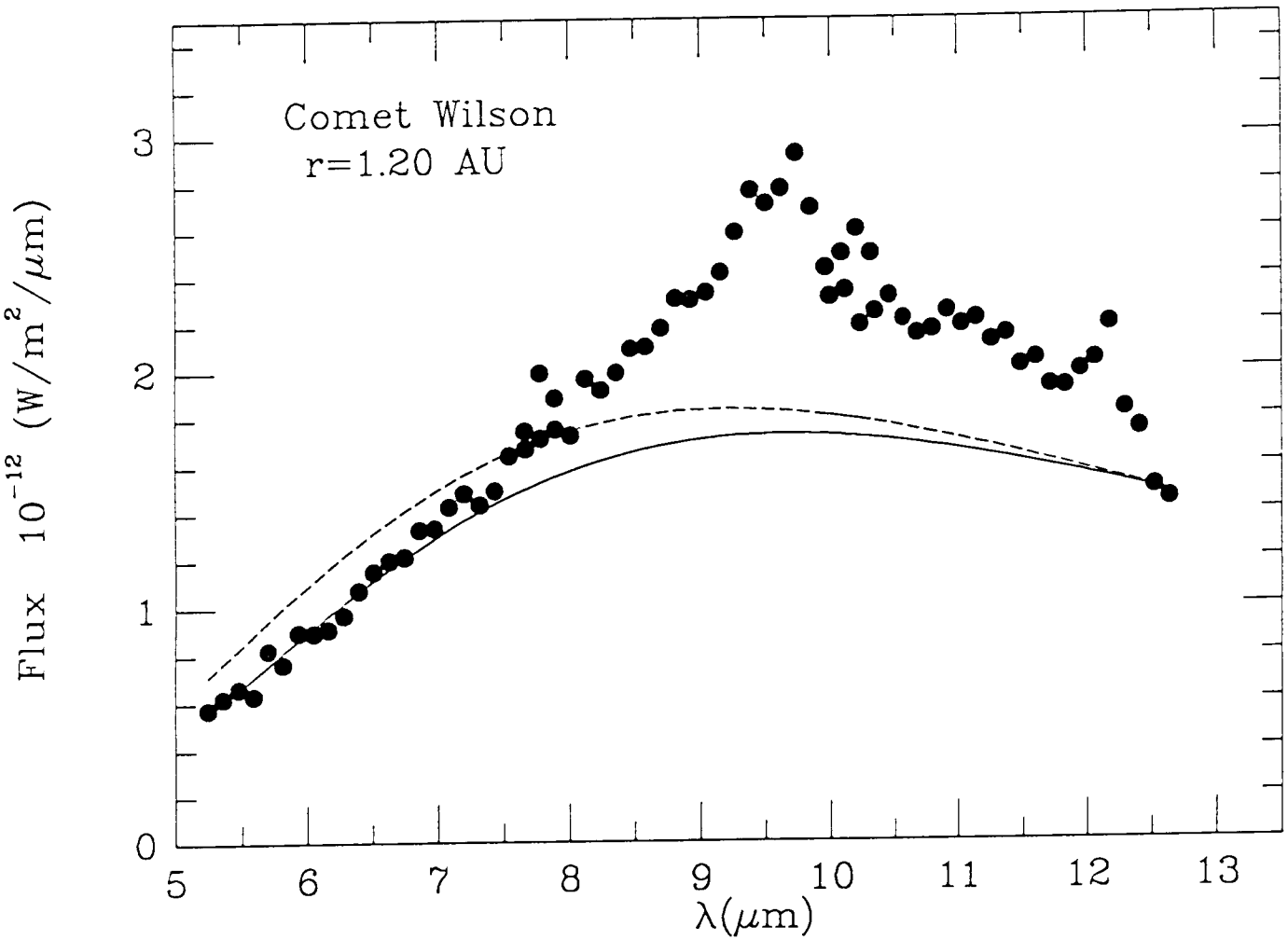
Comet Wilson
r=1.20 AU
Flux 10^{-12} (W/m^2/μm)
$\lambda(\mu m)$
0
1
2
3
5
6
7
8
9
10
11
12
13

Fig. 1e

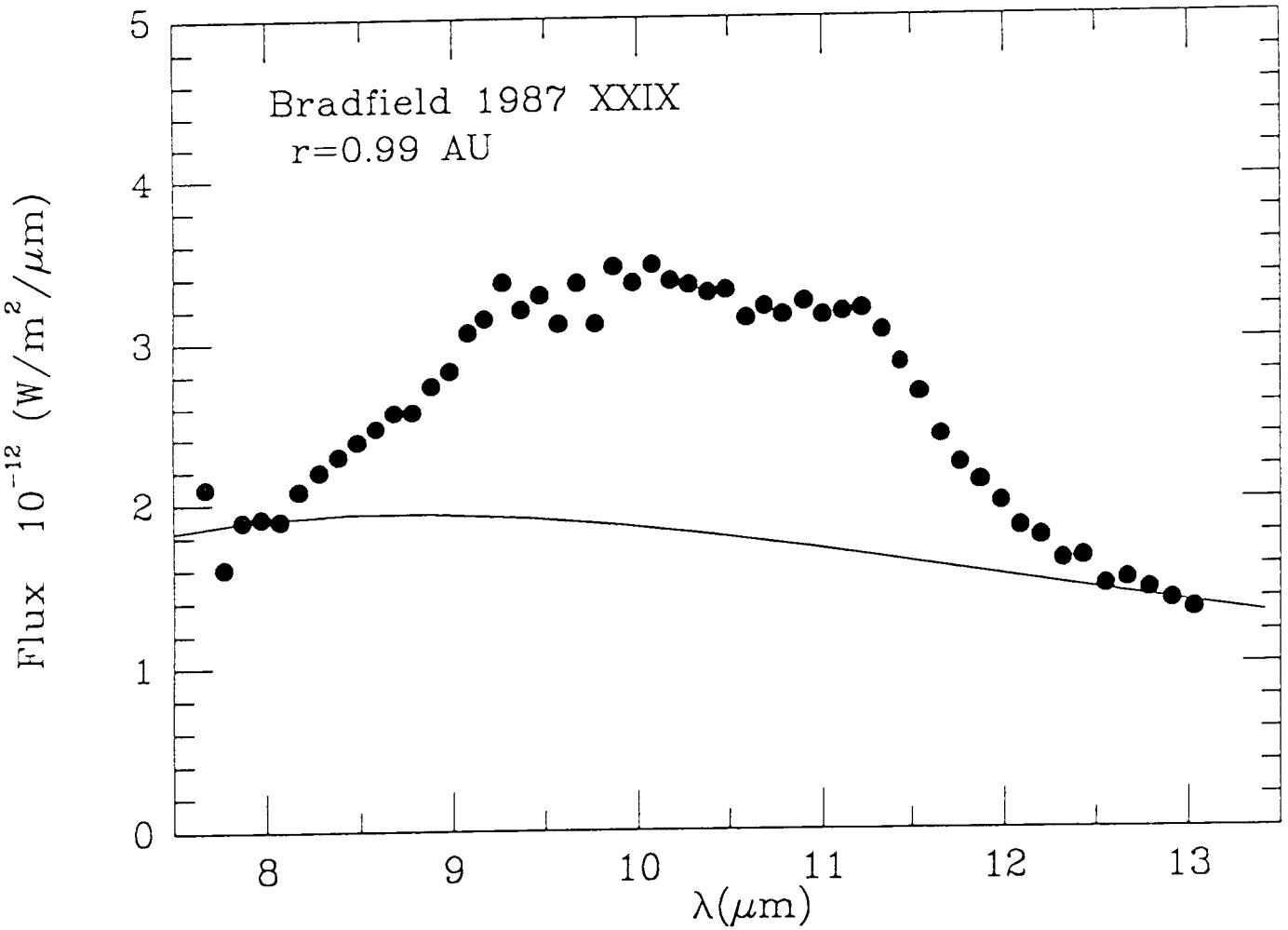
Bradfield 1987 XXIX
r=0.99 AU
Flux 10^{-12} (W/m^2/μm)
$\lambda(\mu m)$
0
1
2
3
4
5
8
9
10
11
12
13

Fig. 1f

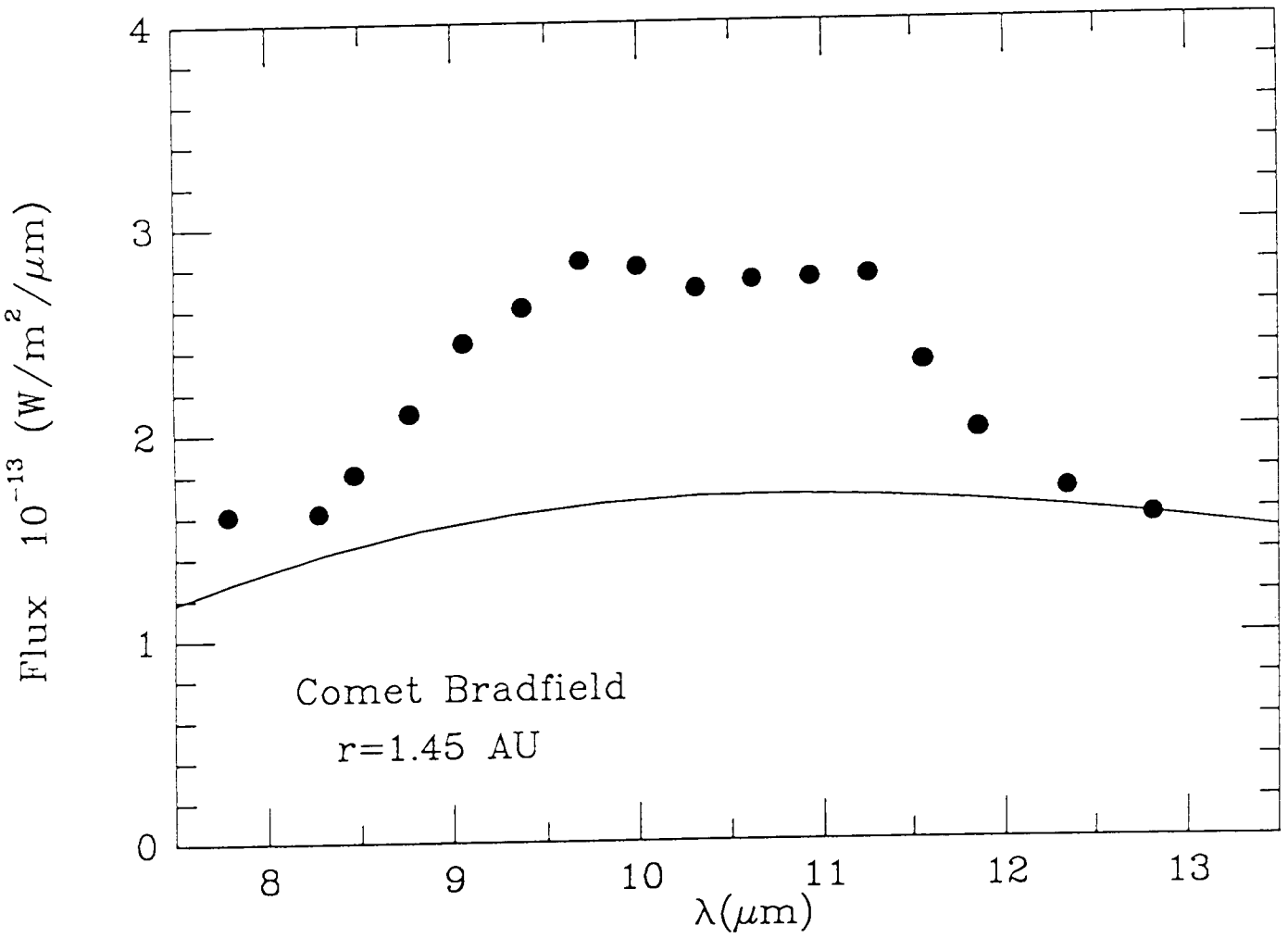
Flux 10^{-13} (W/m^2/μm)
4
3
2
1
0
8
9
10
11
12
13
$\lambda(\mu m)$
Comet Bradfield
r=1.45 AU

Fig. 4a

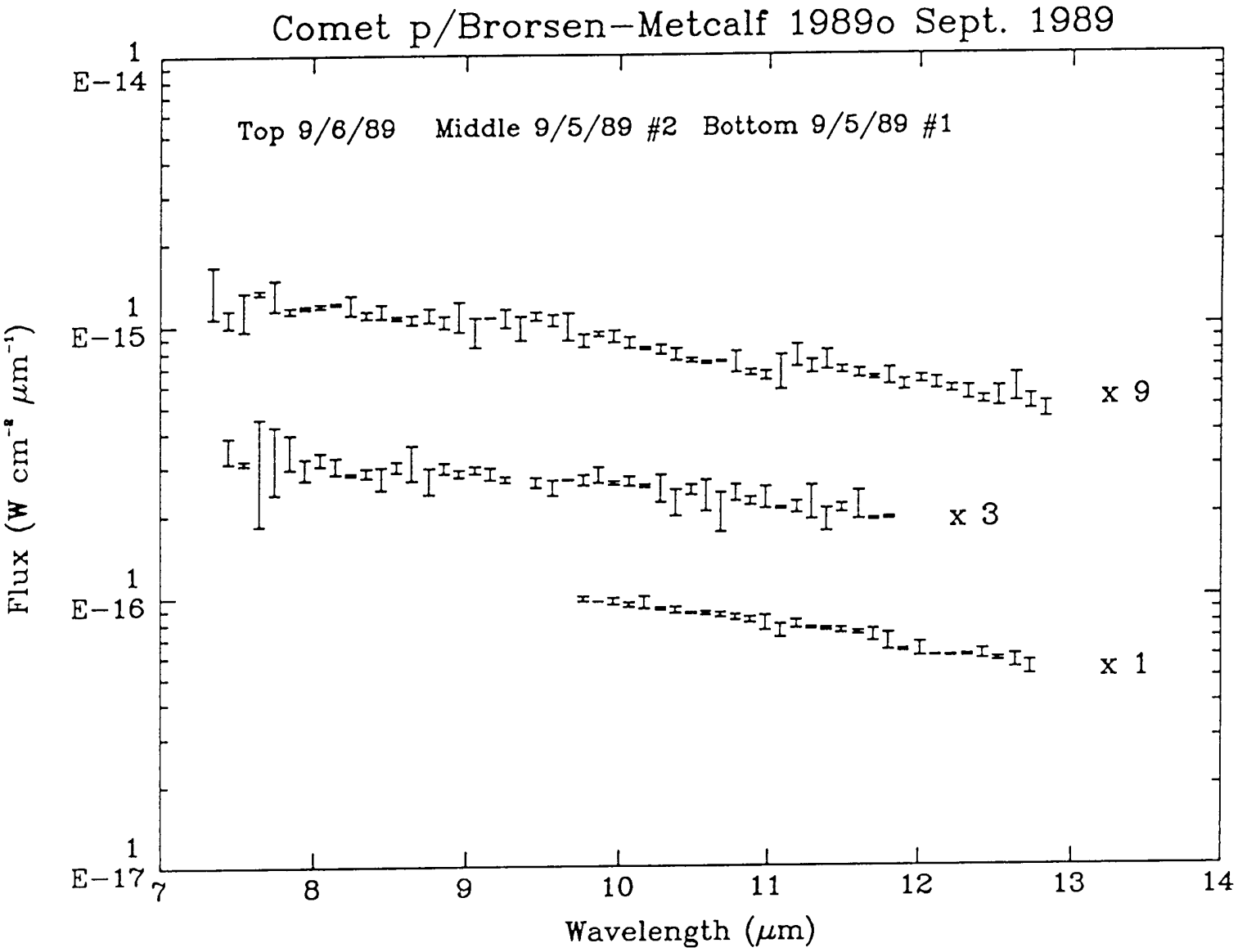
Comet p/Brorsen–Metcalf 1989o Sept. 1989
Top 9/6/89 Middle 9/5/89 #2 Bottom 9/5/89 #1
x 9
x 3
x 1
Flux (W cm⁻² μm⁻¹)
1 E−14
1 E−15
1 E−16
1 E−17
7
8
9
10
11
12
13
14
Wavelength (μm)

Fig. 1b

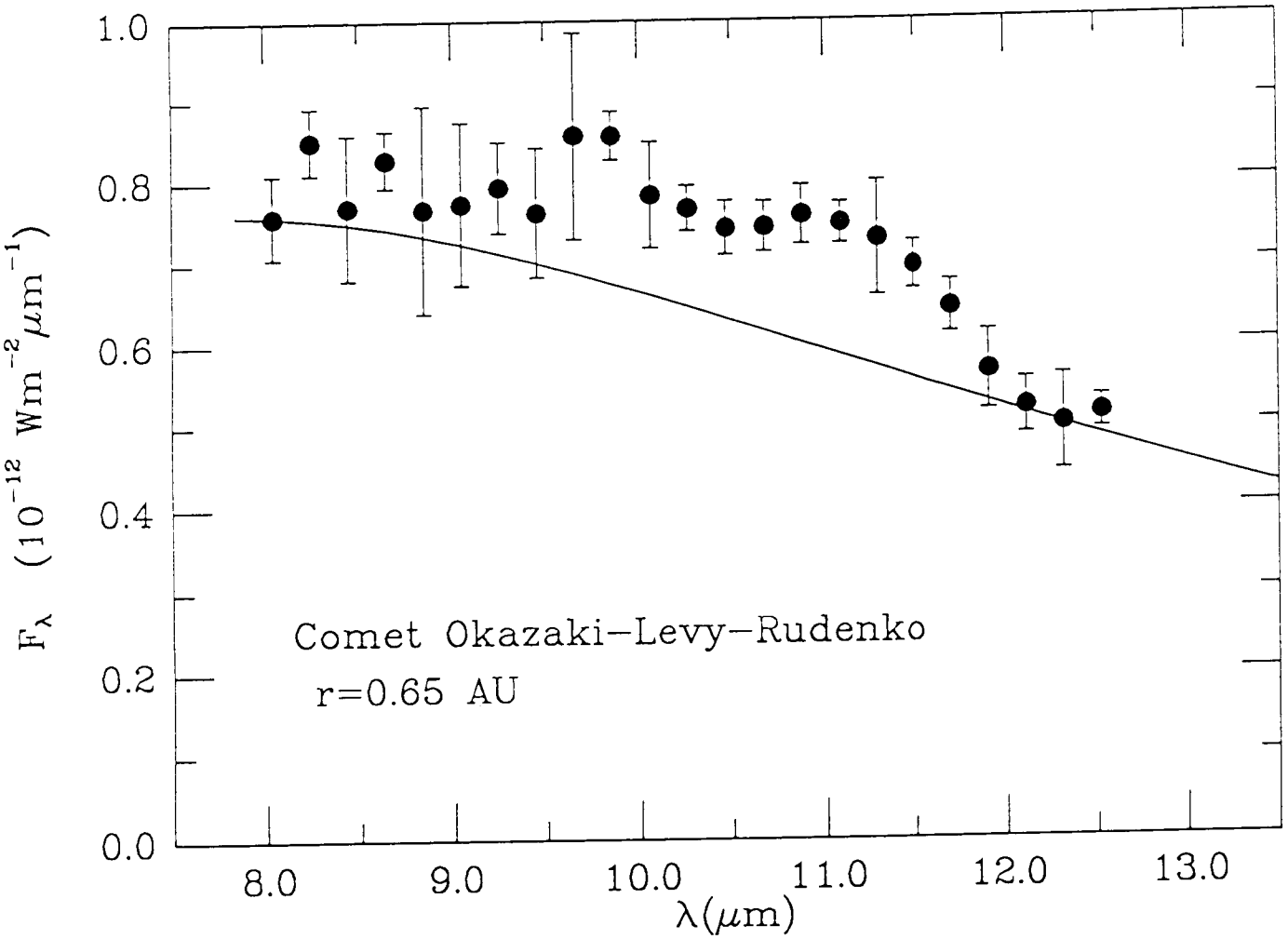
1.0
0.8
0.6
0.4
0.2
0.0
F_λ (10^{-12} $Wm^{-2}\mu m^{-1}$)
Comet Okazaki-Levy-Rudenko
r=0.65 AU
8.0
9.0
10.0
11.0
12.0
13.0
$\lambda(\mu m)$

Fig. 2a

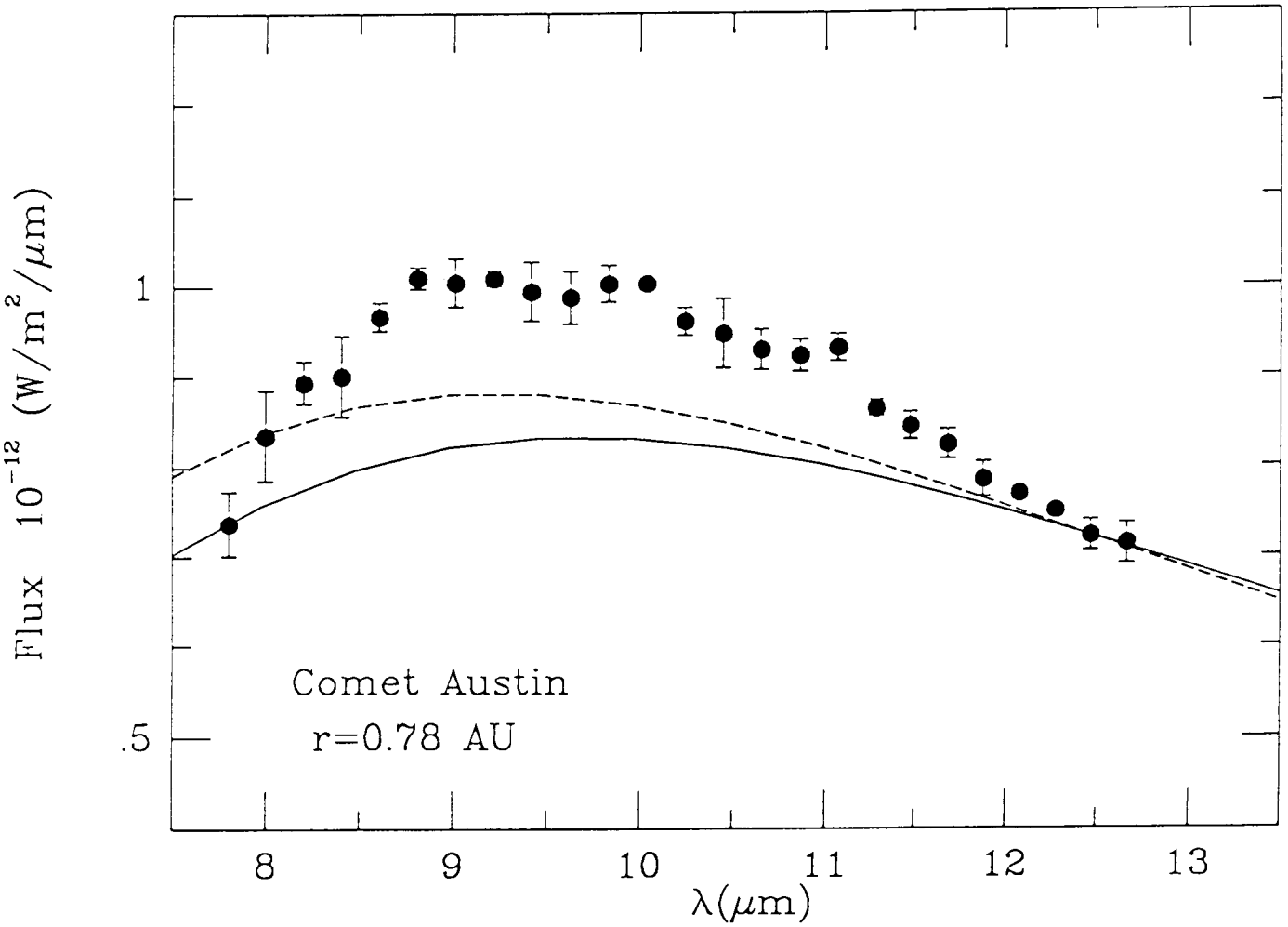
Flux 10^{-12} (W/m^2/μm)
1
.5
Comet Austin
r=0.78 AU
8
9
10
11
12
13
$\lambda(\mu m)$

Fig. 4

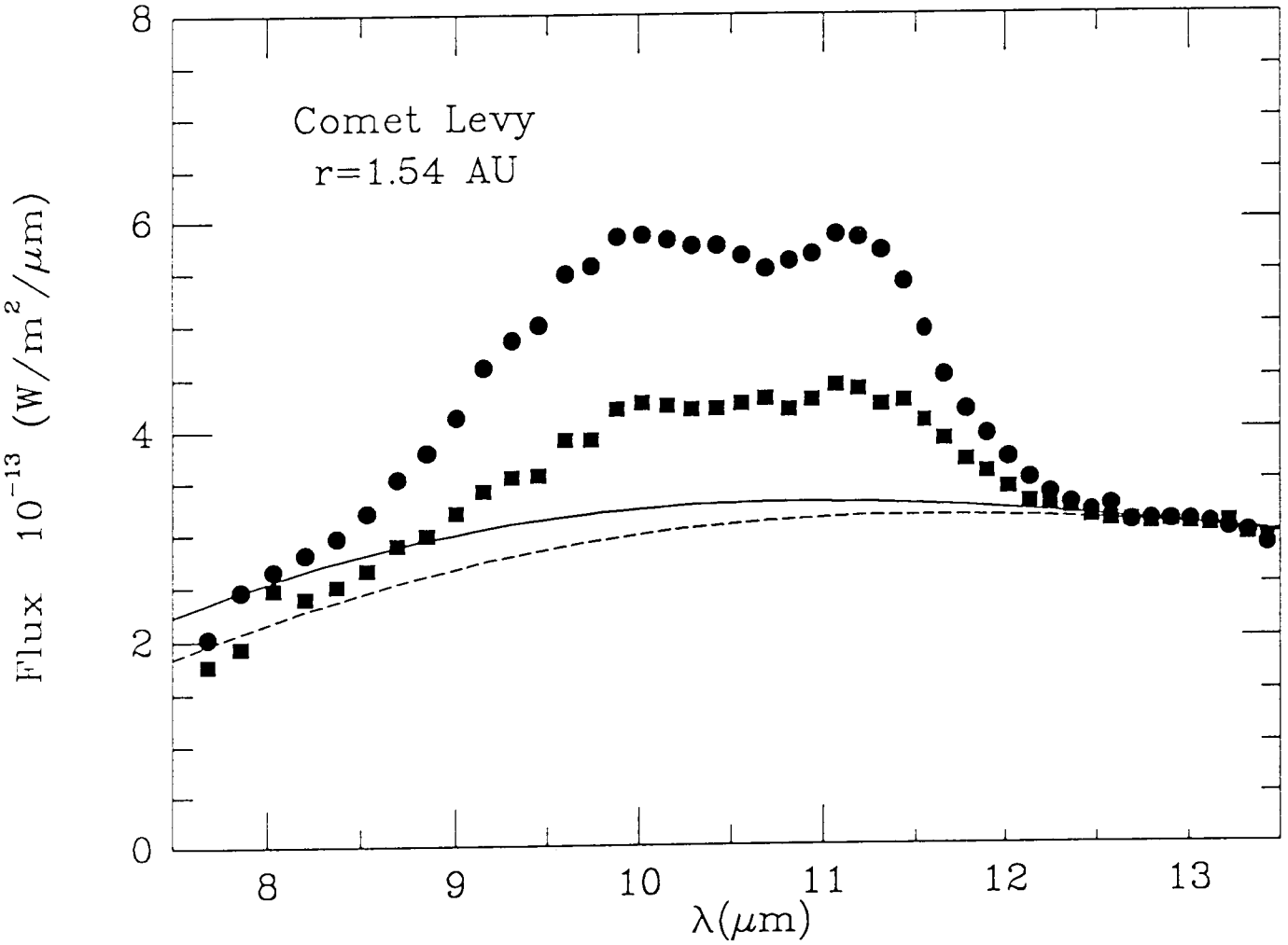
Comet Levy
r=1.54 AU
Flux 10^{-13} (W/m^2/μm)
$\lambda(\mu m)$
0
2
4
6
8
8
9
10
11
12
13

Fig. 1k

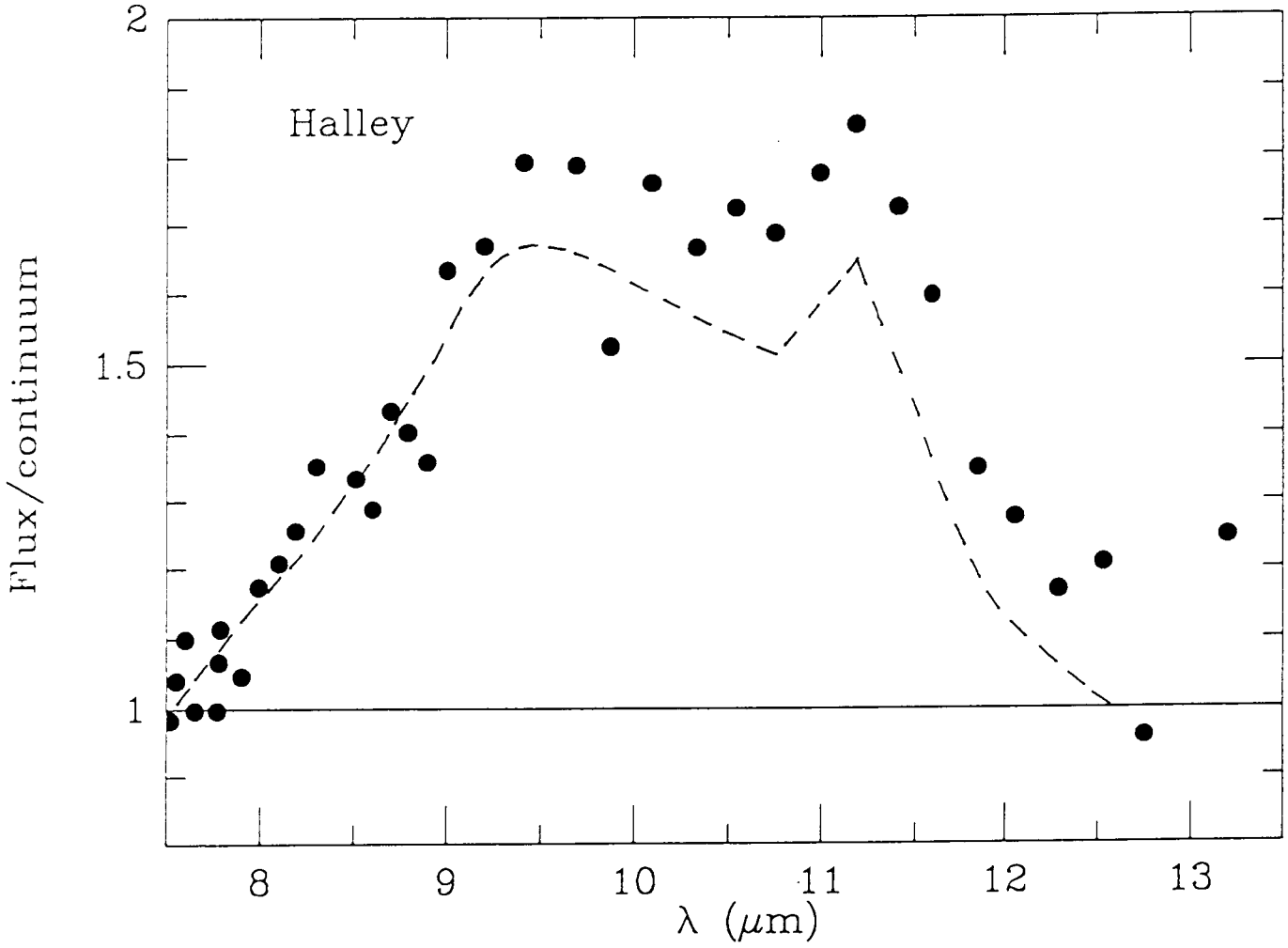

Fig. 23

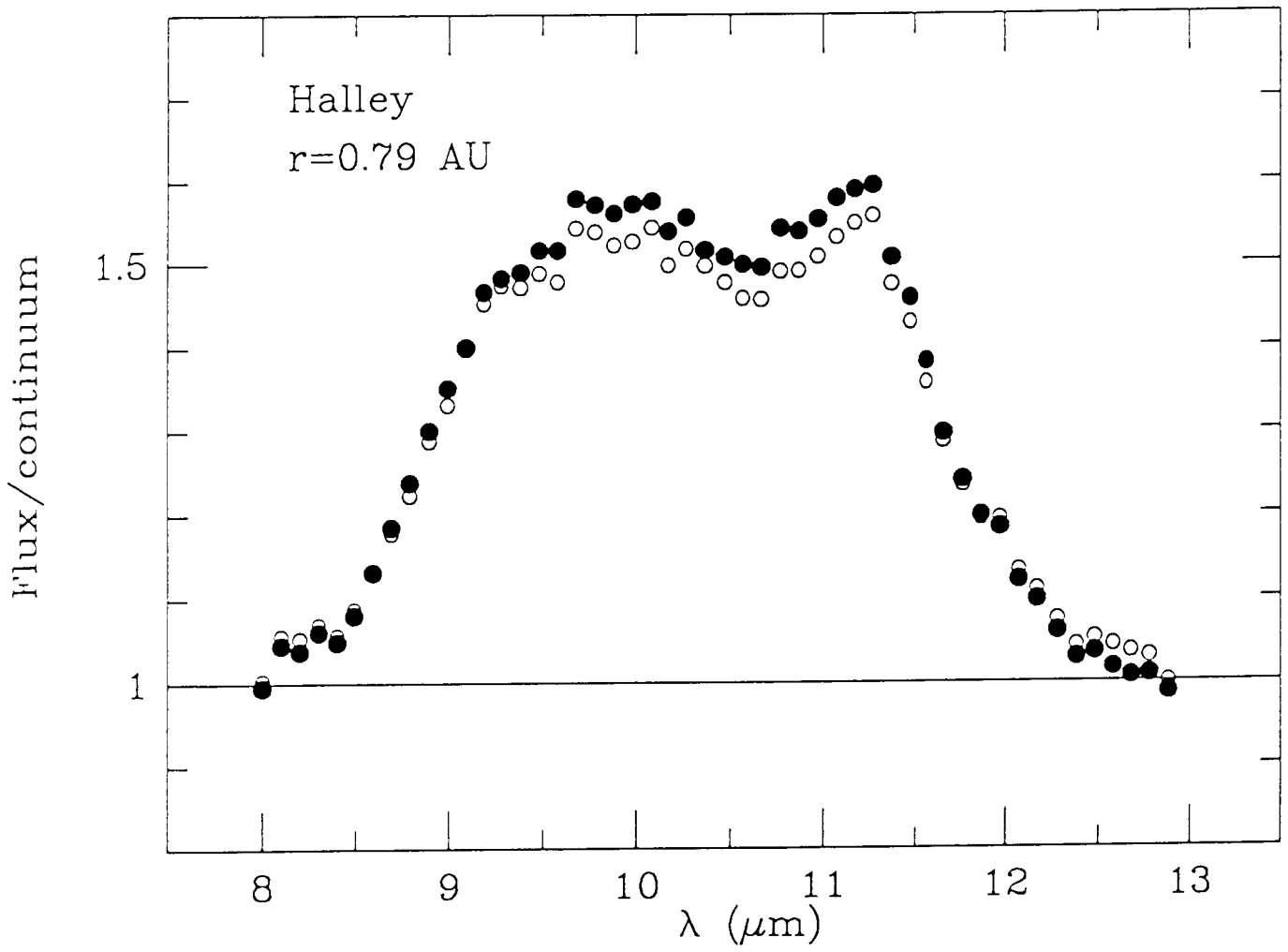

Fig. 2b

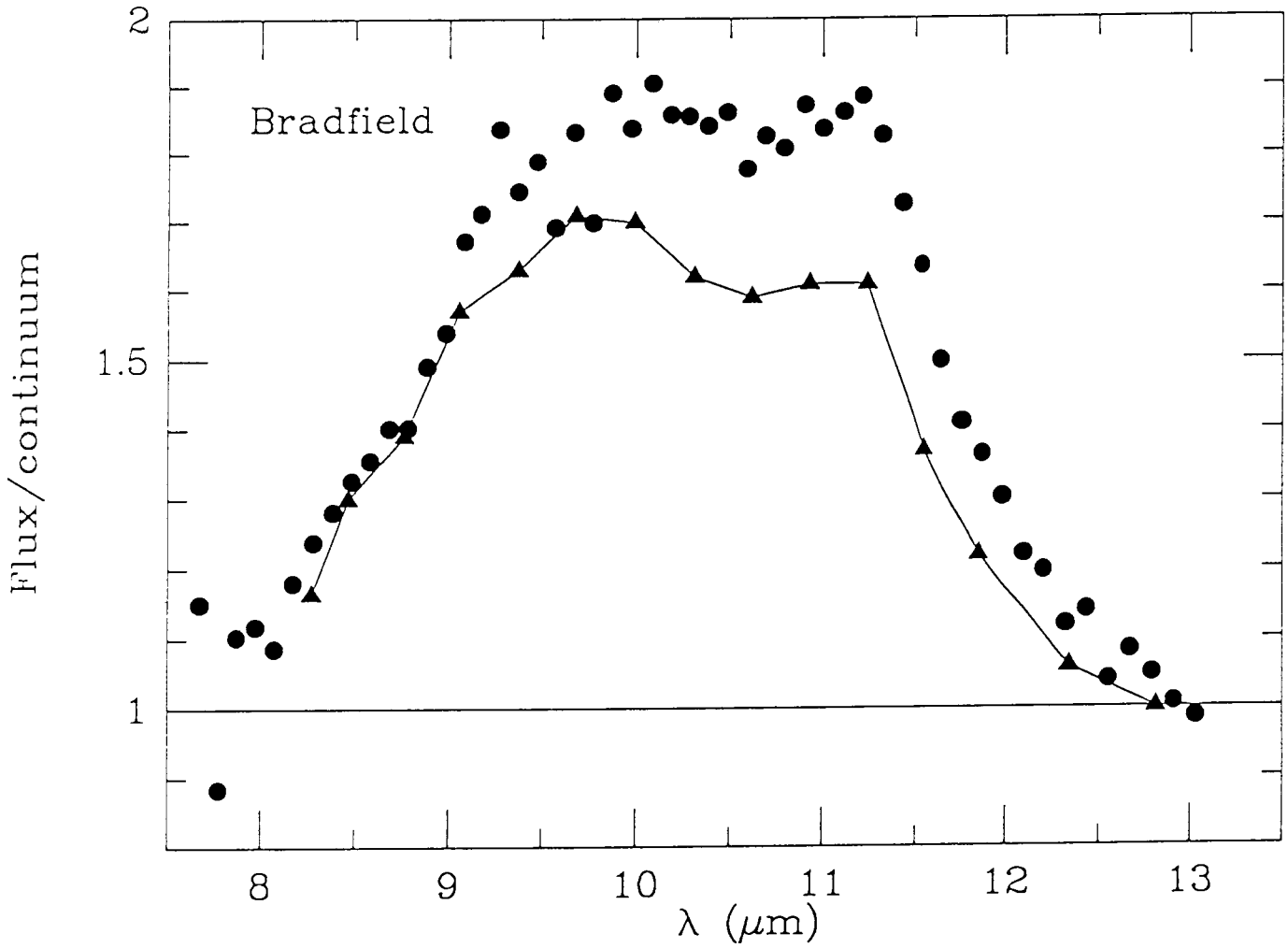

Fig. 23

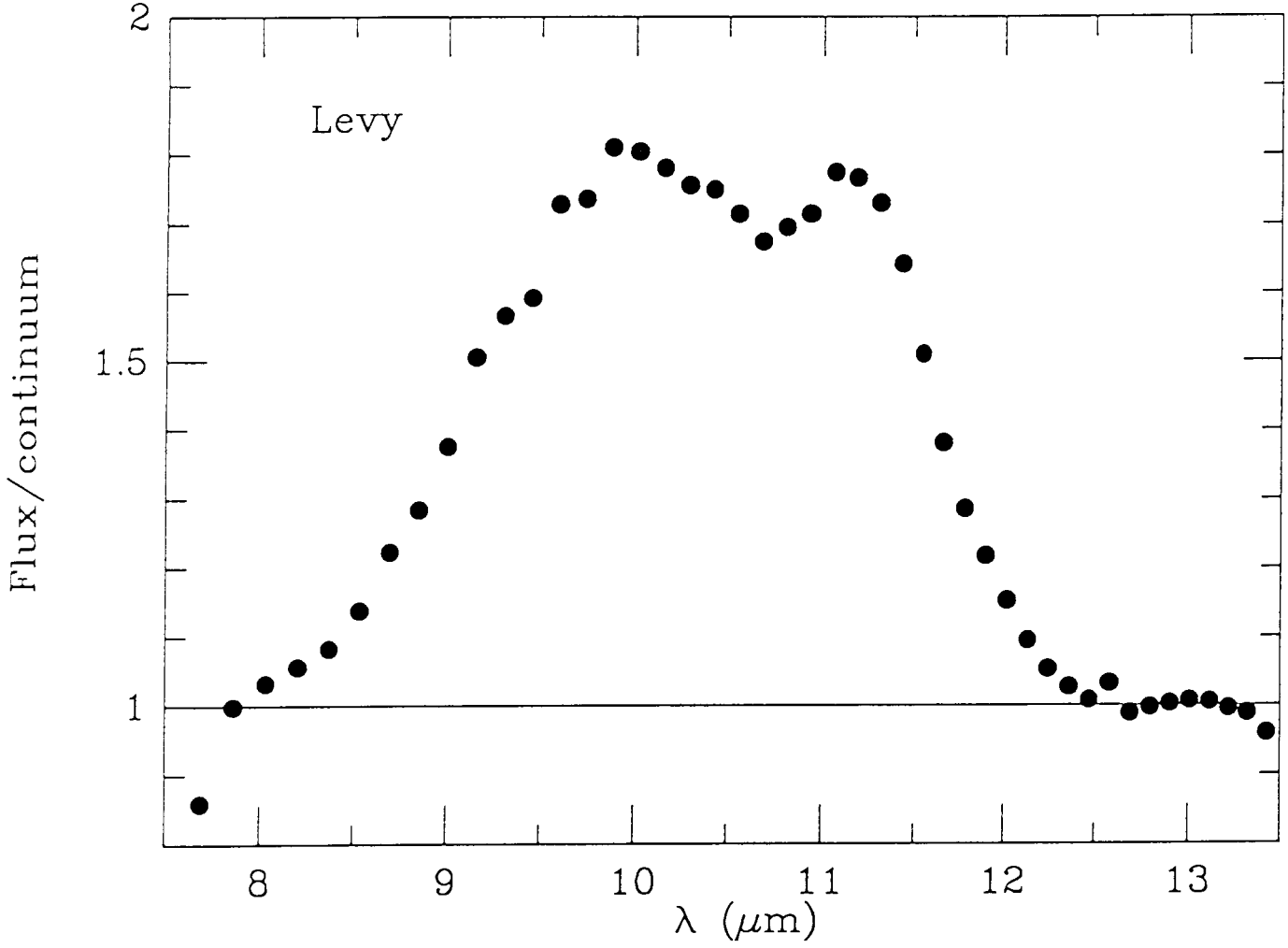

Fig. 2d

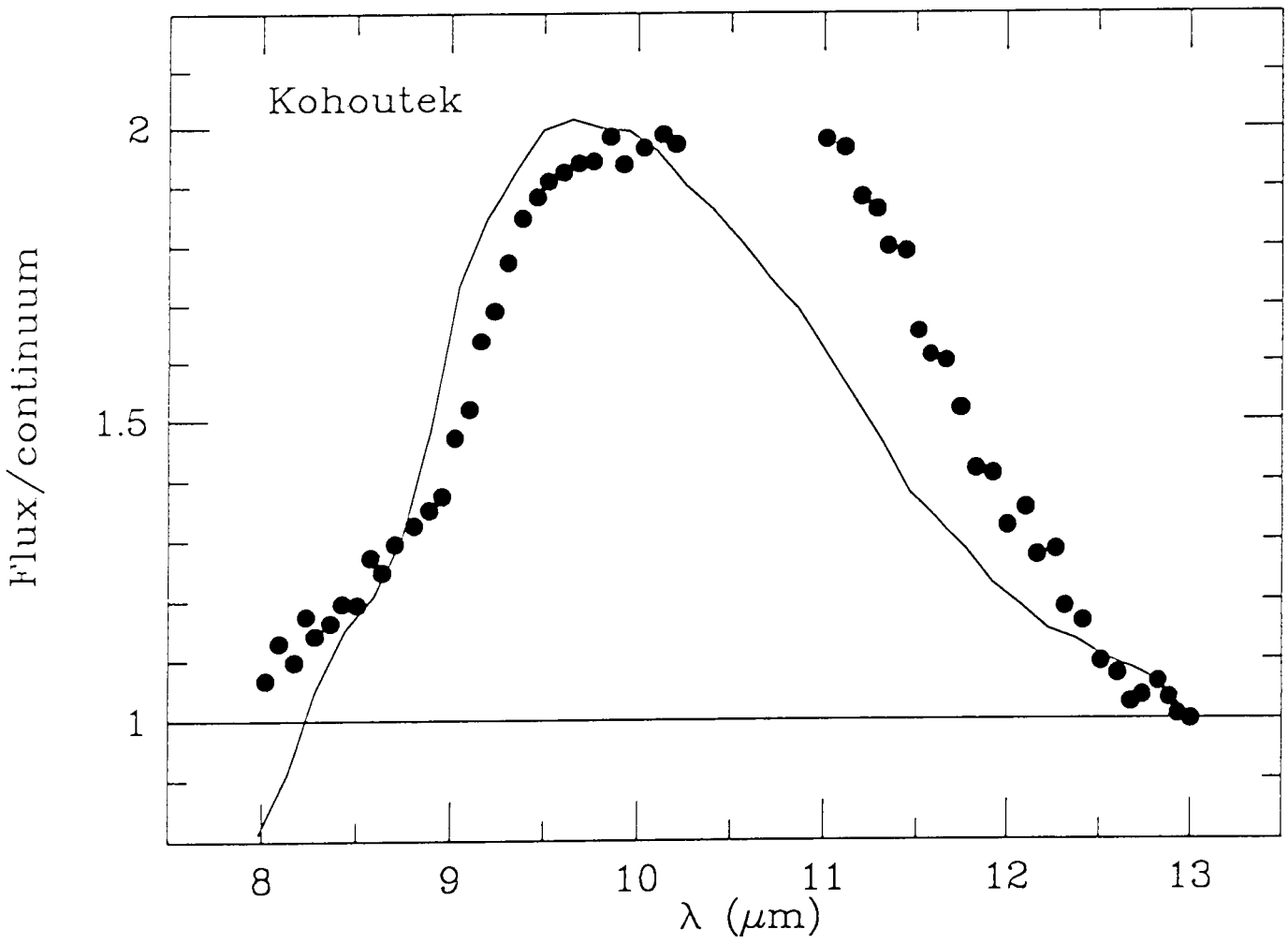

Fig. 2e

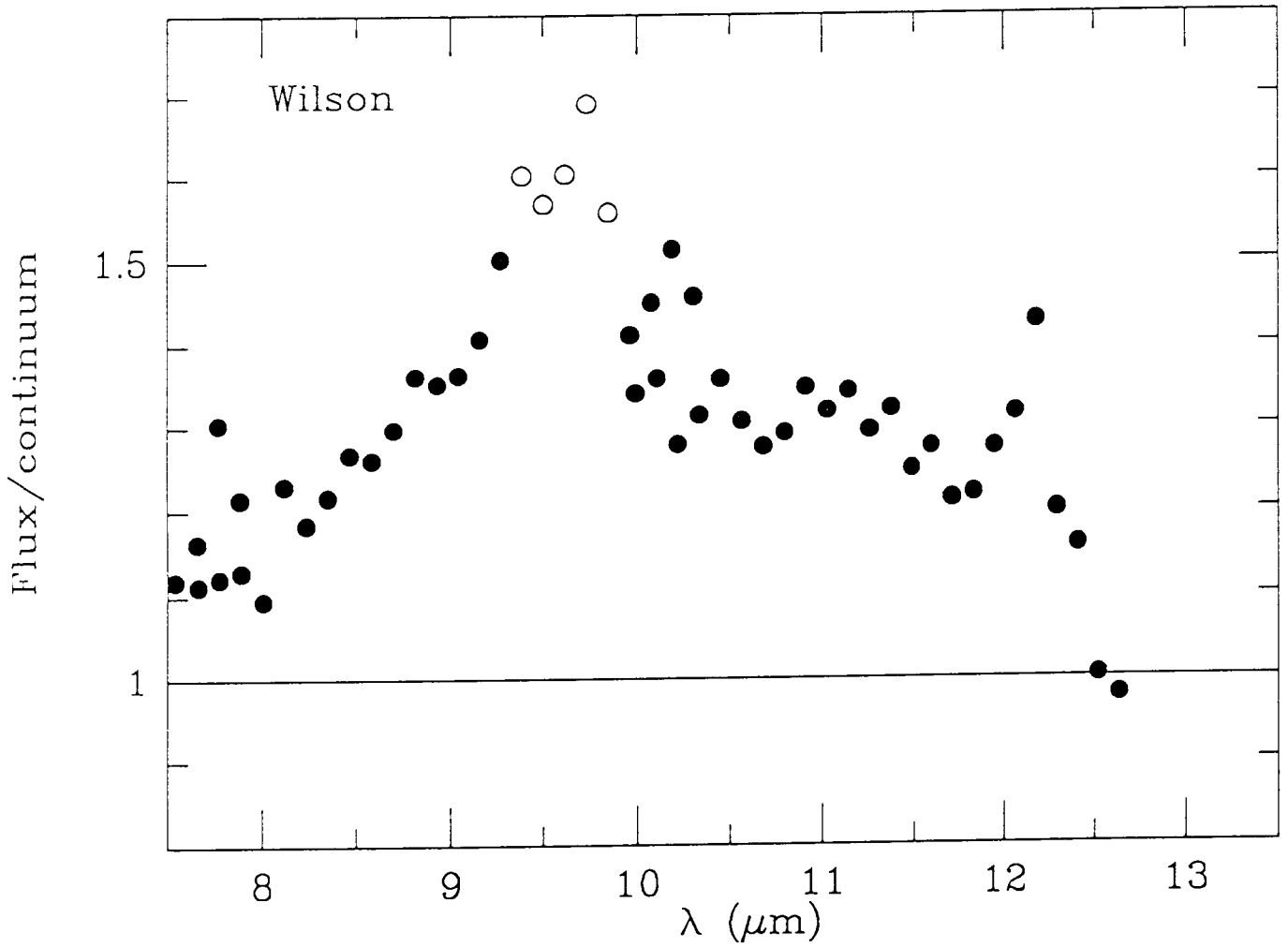

Fig. 2F

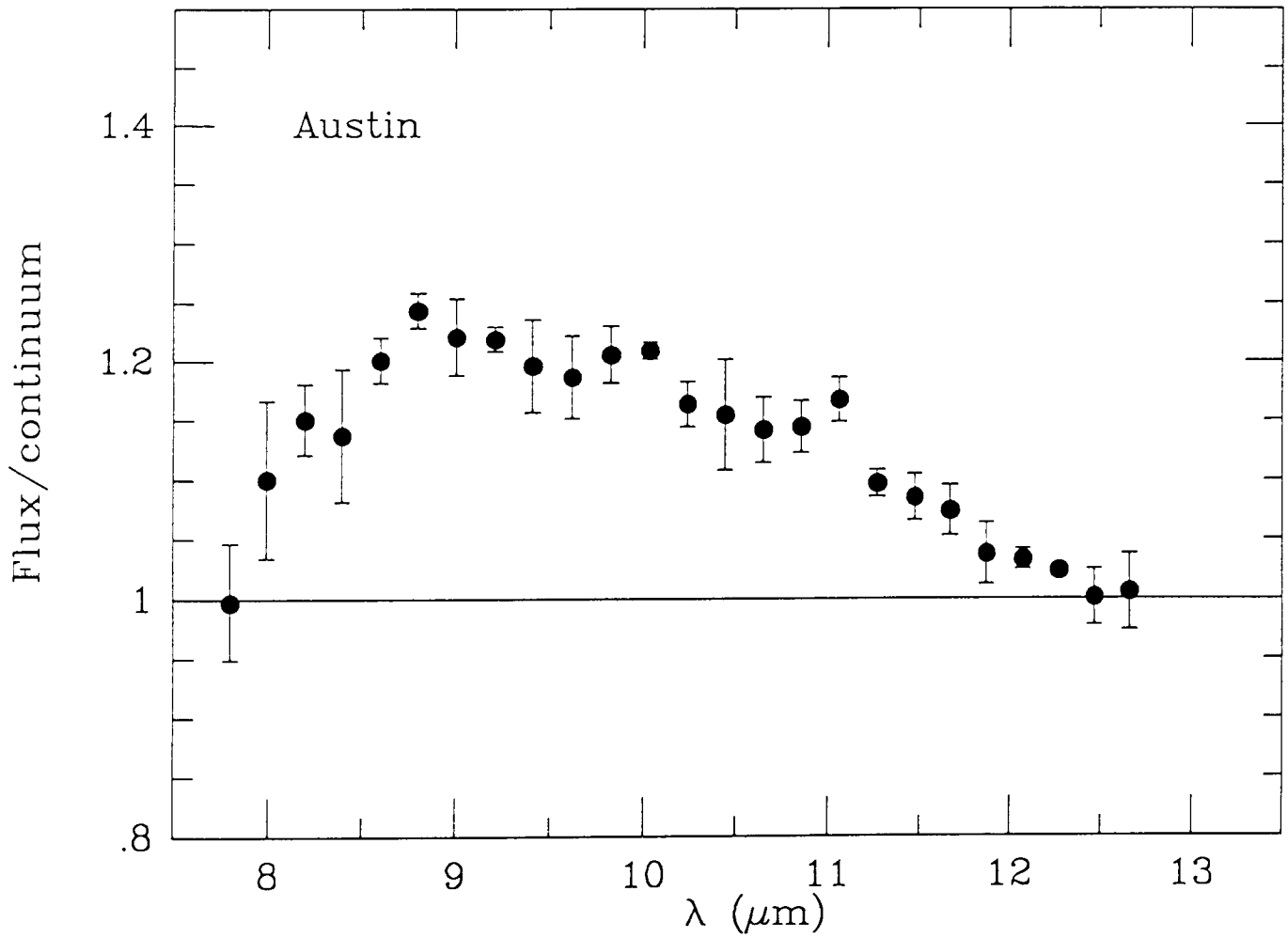

Fig. 2g

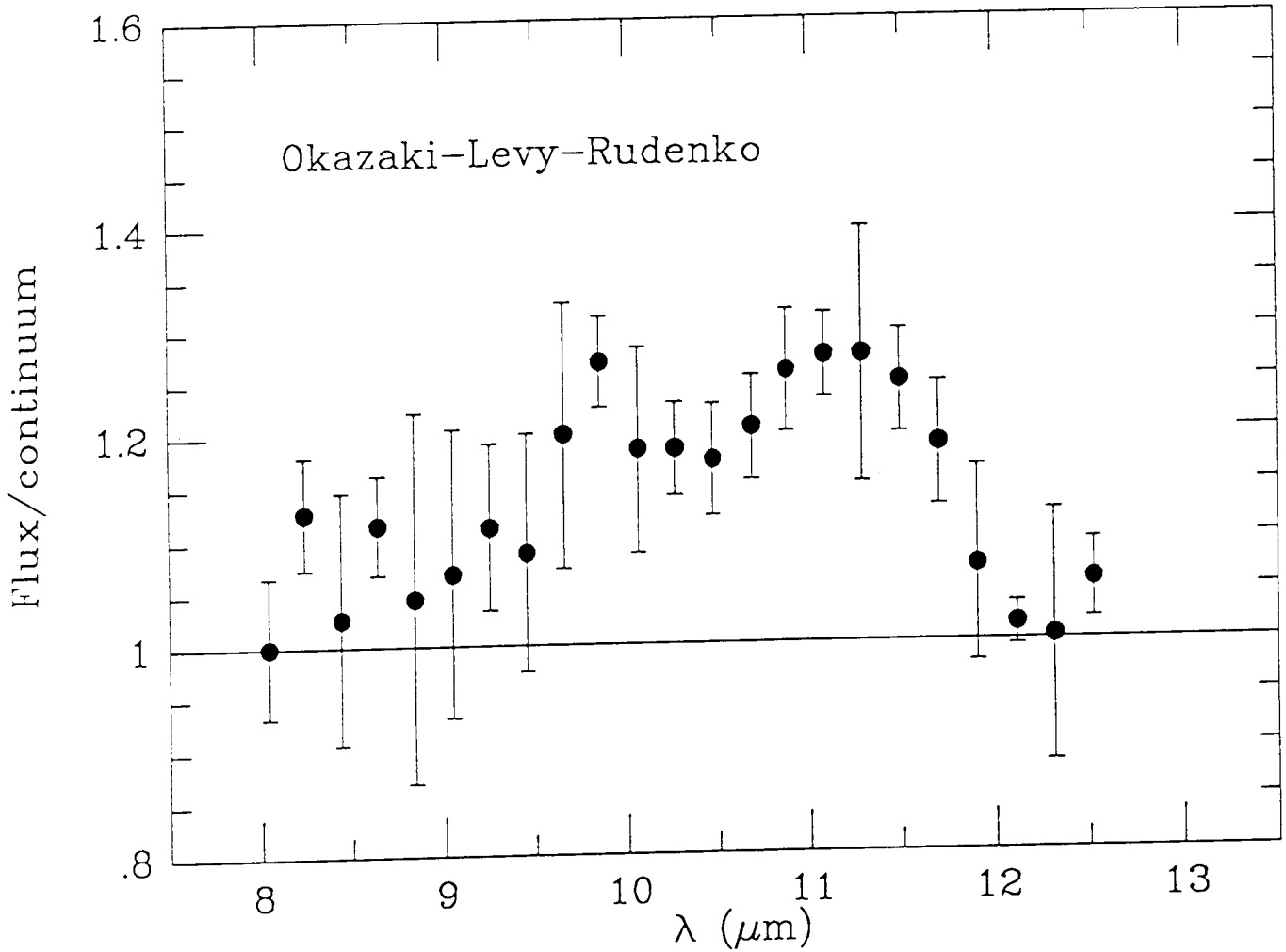
Okazaki–Levy–Rudenko
Flux/continuum
λ (μm)
1.6
1.4
1.2
1
.8
8
9
10
11
12
13

Fig. 2h

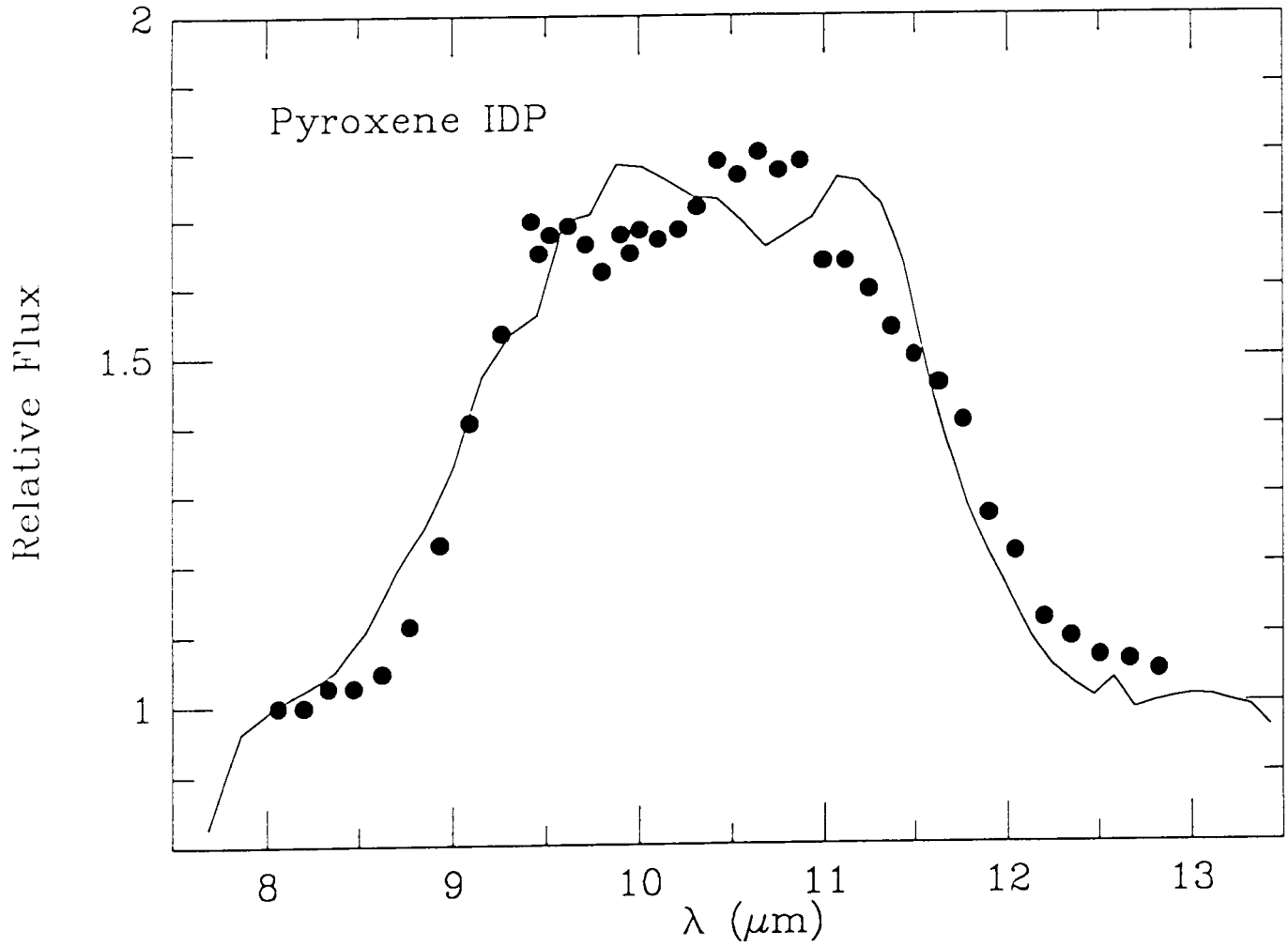
Pyroxene IDP
Relative Flux
2
1.5
1
8
9
10
11
12
13
λ (μm)

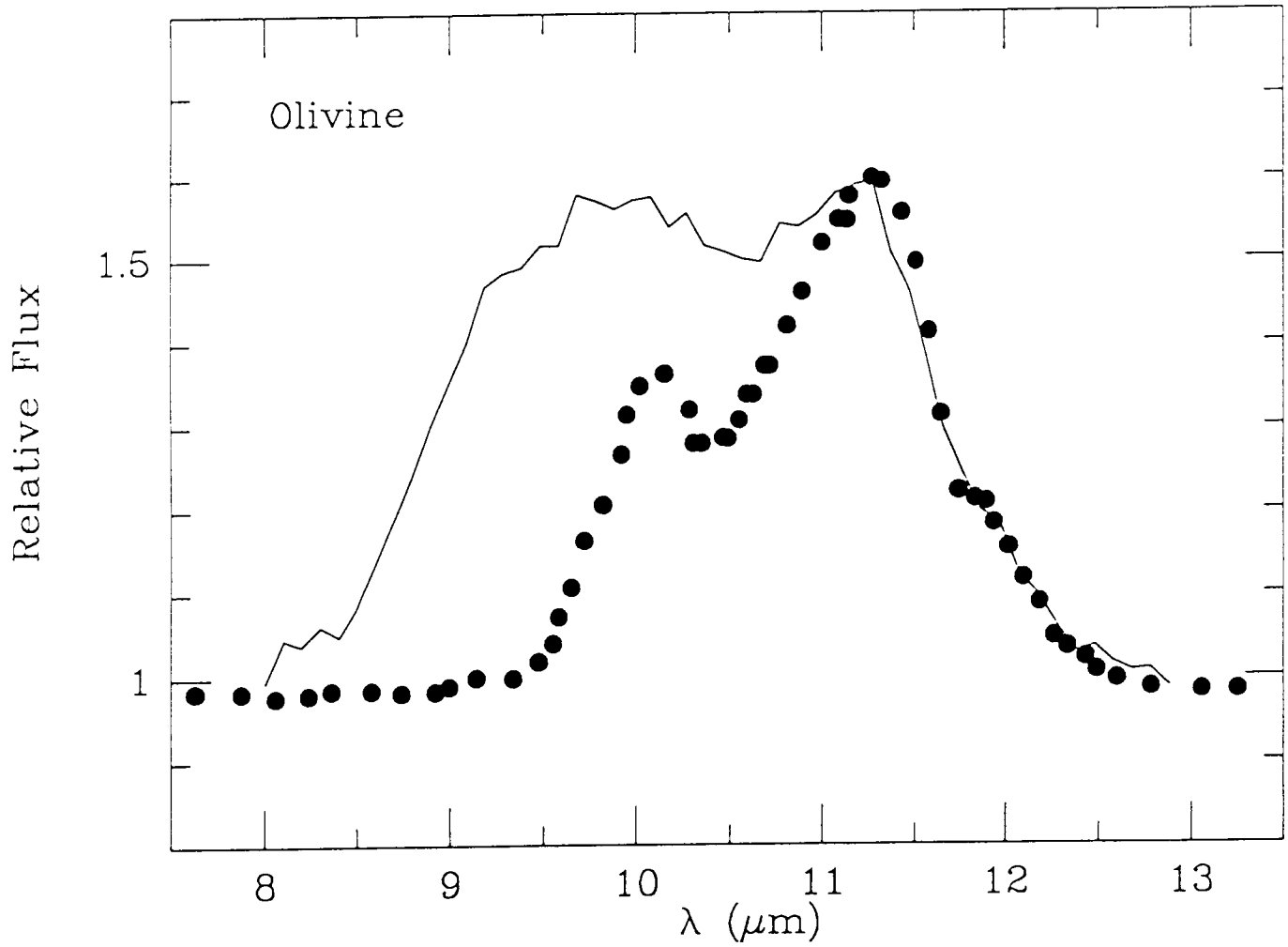
Olivine
Relative Flux
1.5
1
8
9
10
11
12
13
λ (μm)

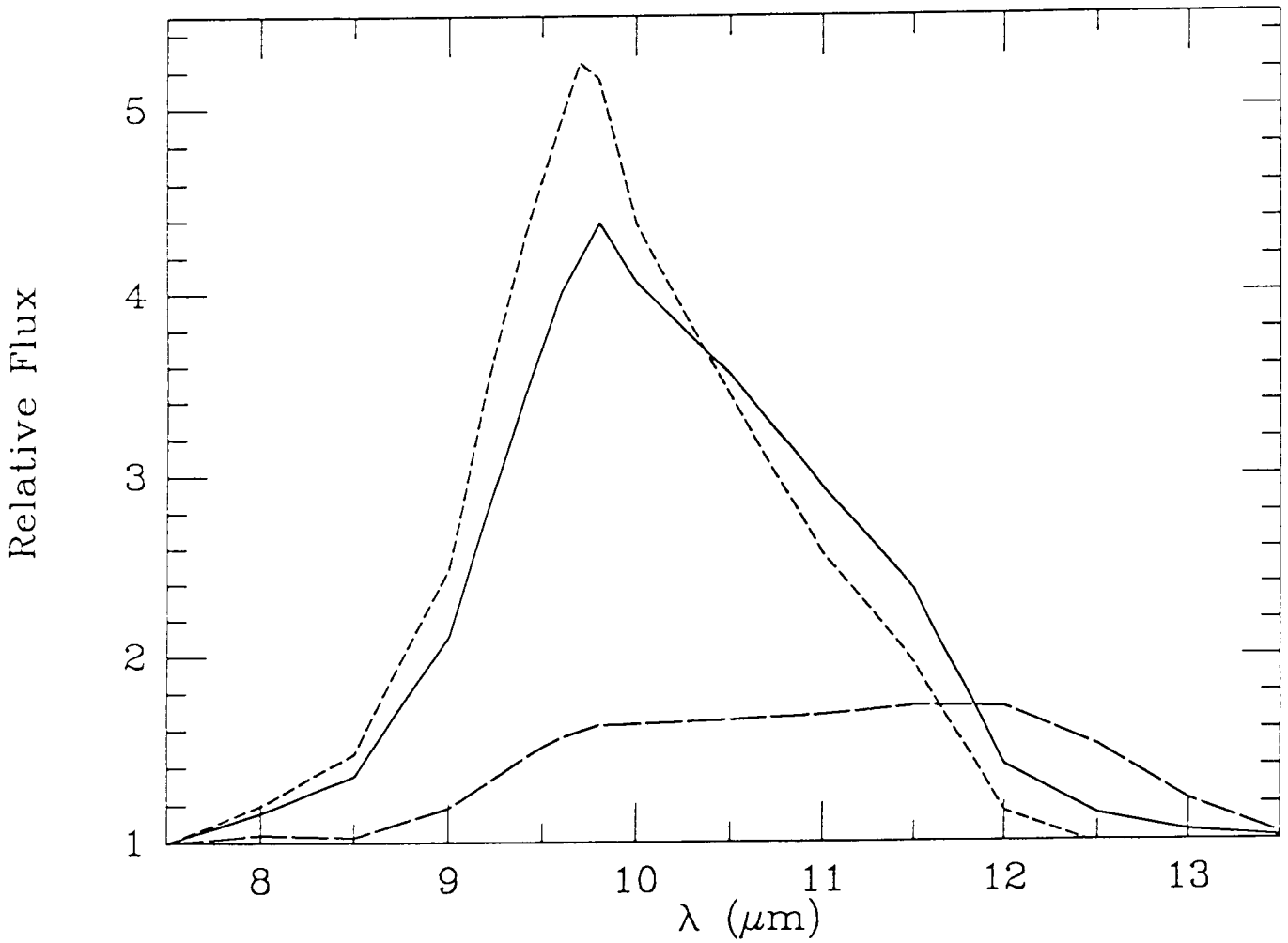
Relative Flux
1
2
3
4
5
8
9
10
11
12
13
λ (μm)

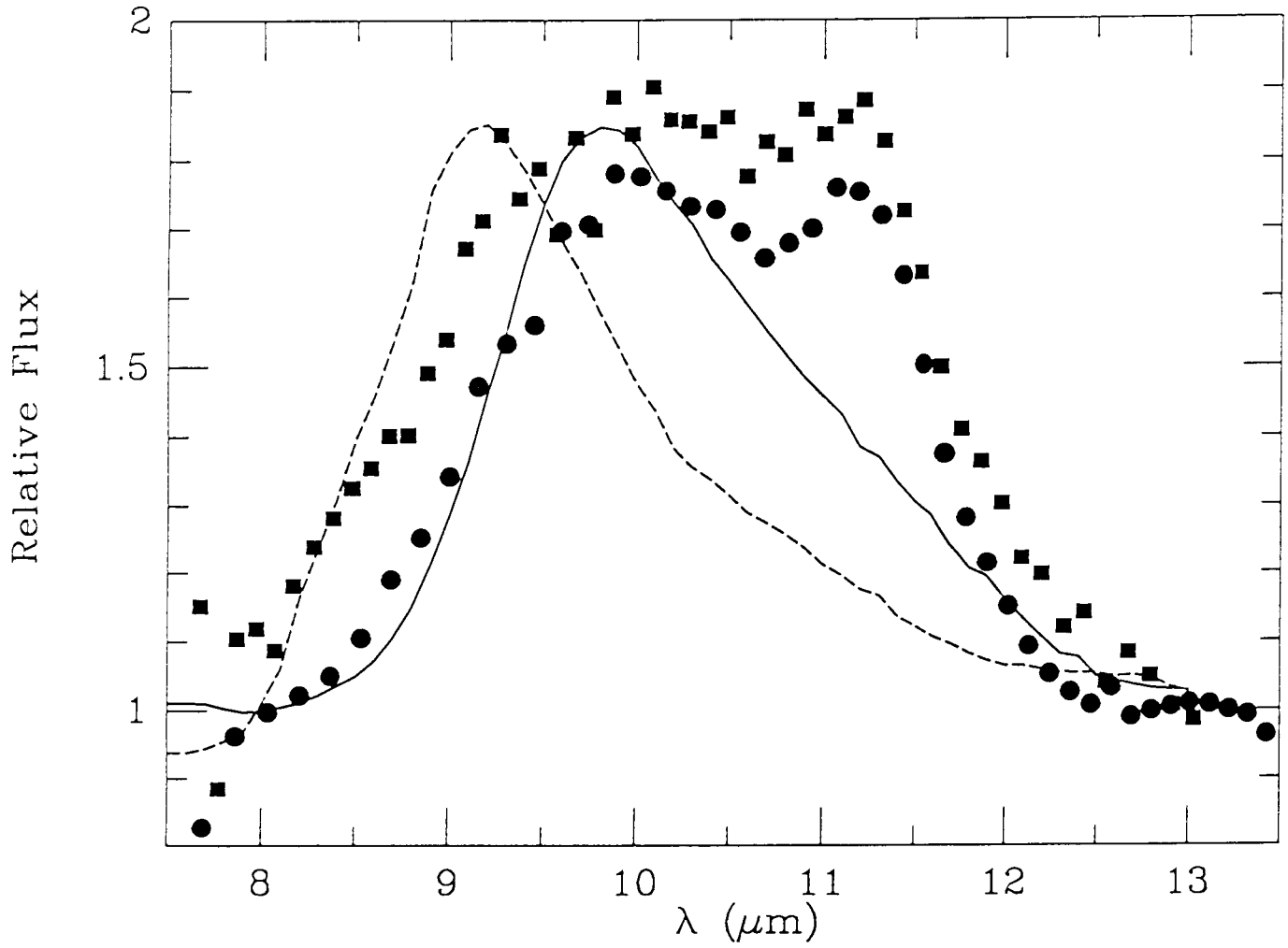
2
1.5
1
Relative Flux
8
9
10
11
12
13
λ (μm)

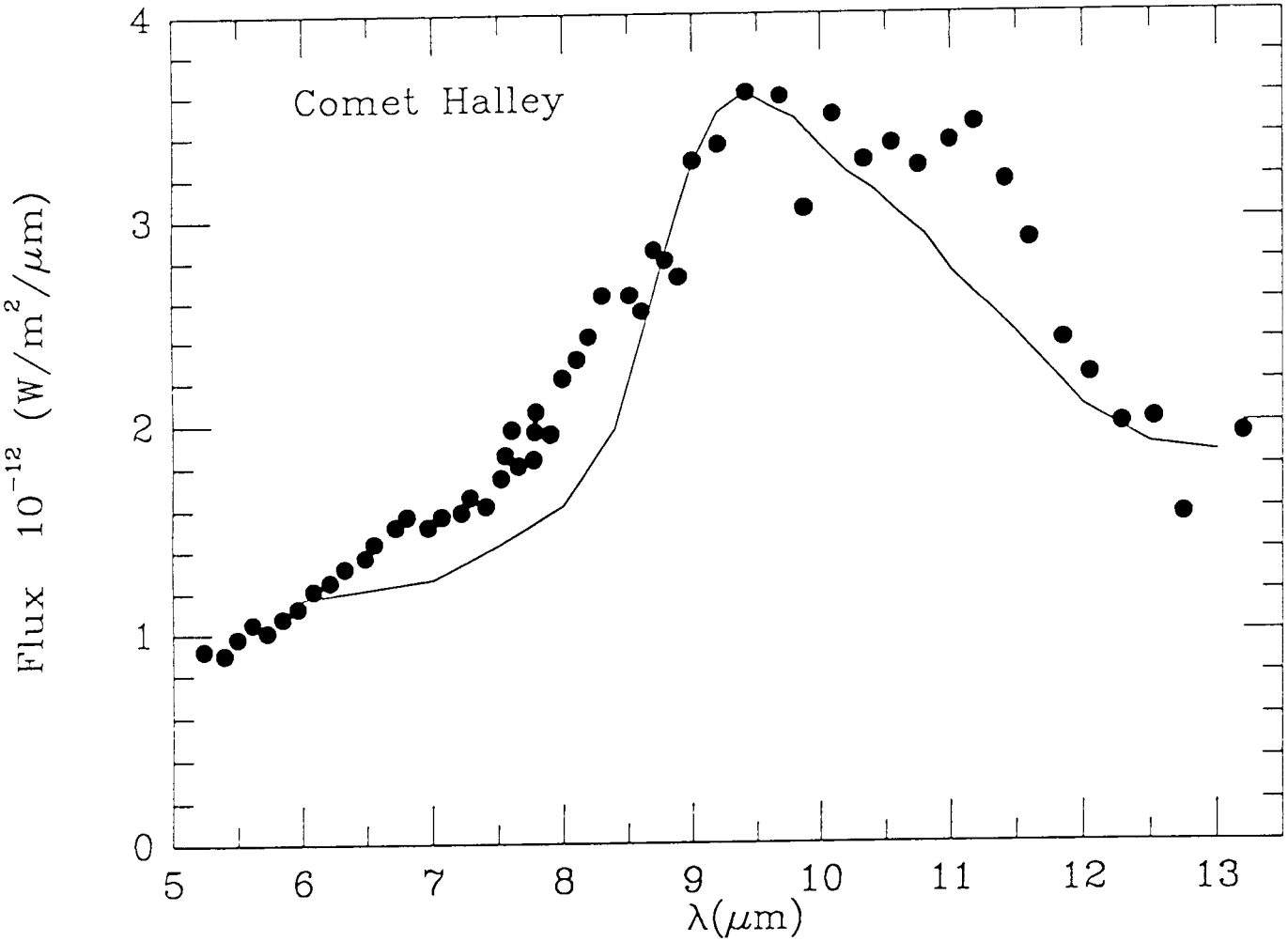
Comet Halley
Flux 10^{-12} (W/m^2/μm)
$\lambda(\mu m)$
0
1
2
3
4
5
6
7
8
9
10
11
12
13

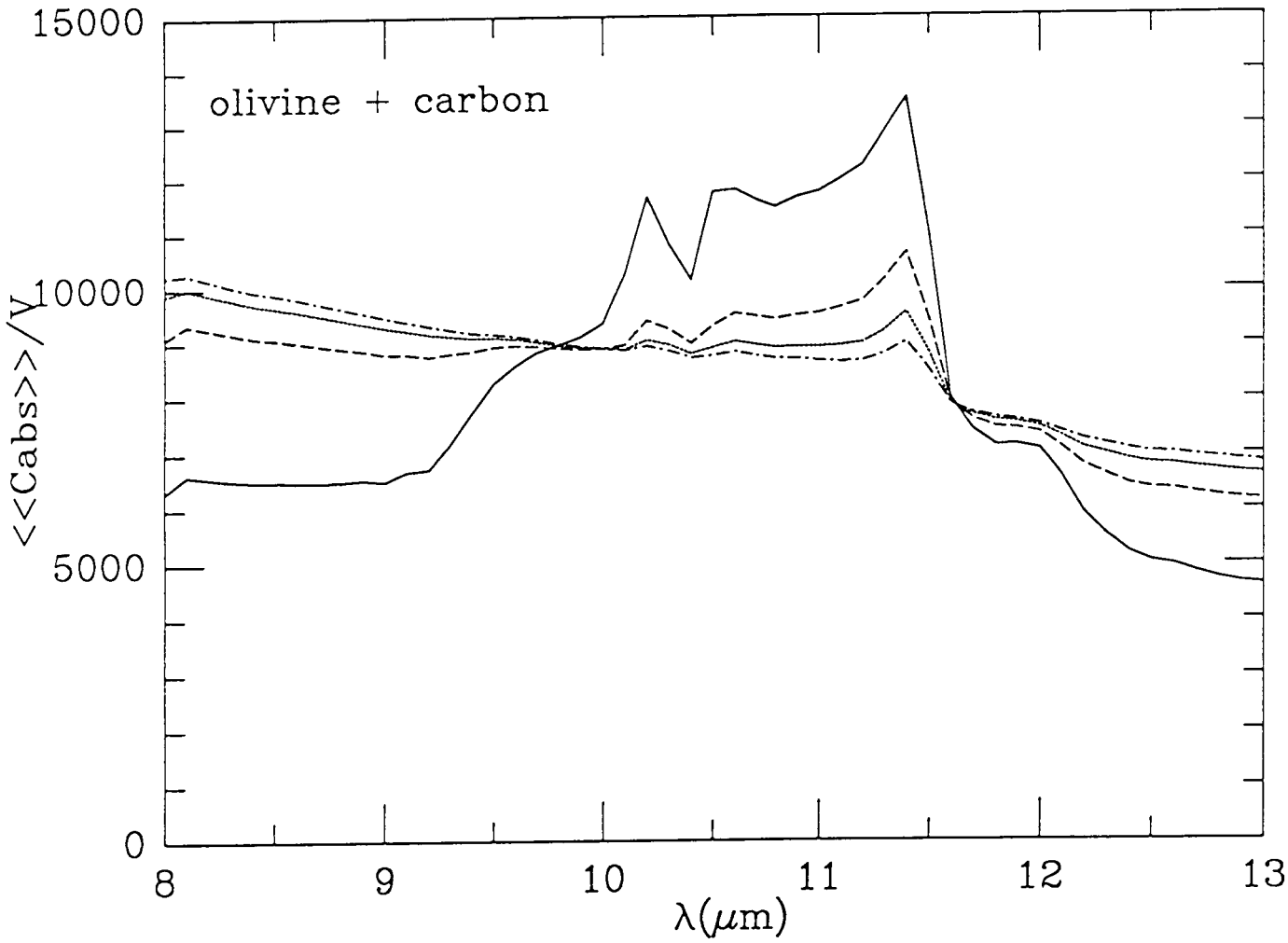
olivine + carbon
15000
10000
5000
0
<<Cabs>>/V
8
9
10
11
12
13
λ(μm)

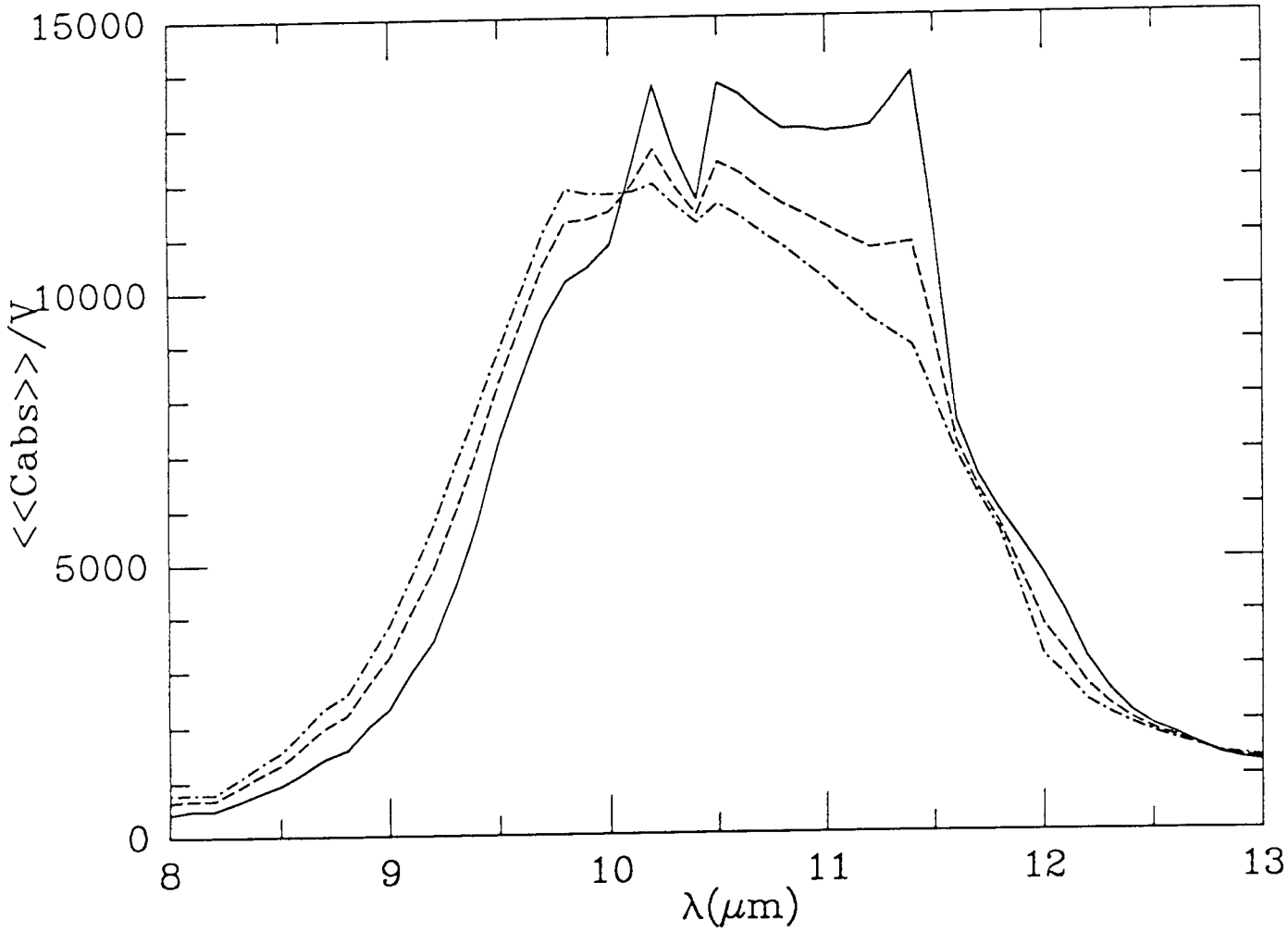
15000
10000
5000
0
<<Cabs>>/V
8
9
10
11
12
13
λ(μm)